

COMBINATORIAL CONNECTIONS IN SNAKE GRAPHS: TILINGS, LATTICE PATHS, AND PERFECT MATCHINGS

CAROLINA MELO

ABSTRACT. This paper delves into the combinatorial structures underlying snake graphs, focusing on their connections to domino tilings, lattice paths, and perfect matchings. By exploring the structure of snake graphs and their associated regions, we introduce triangular snake graphs (connected acyclic directed graphs) and provide a bijection between their routes (non-intersecting lattice paths), perfect matchings of their underlying snake graphs, and tilings, revealing significant relationships and identities.

Furthermore, we study the algebraic implications of these combinatorial structures. We show how the number of perfect matchings in snake graphs can be expressed in terms of determinants of Hankel matrices or path matrices associated with Catalan, Fibonacci, and Pell numbers. This provides a novel perspective on the interplay between combinatorial objects and algebraic identities.

CONTENTS

1. Introduction	1
1.1. Overview	1
1.2. Organization	4
2. Background	4
2.1. Lattice paths and Aztec diamonds	4
2.2. Hankel matrices and lattice paths	5
2.3. Perfect matchings and snake graphs	7
3. Perfect matchings, tilings and non-intersecting lattice paths	8
3.1. Tilings and snake graphs	8
3.2. Decorated snake graph tilings and paths	10
3.3. Edge contraction in snake graphs	16
4. Fibonacci identities and Hankel matrices	20
4.1. Identities in straight snake graphs	20
4.2. Some identities in not straight snake graphs	26
5. Future work	29
6. Acknowledgments	30
References	30

1. INTRODUCTION

1.1. Overview. Given a region (usually a subset of the Euclidean plane) and a collection of shapes (tiles), a *tiling* of that region is defined as a set of non-overlapping tiles whose union is the region. In recent years, the exploration of tilings within different geometric regions, along with the combinatorial challenges they pose, has become a captivating area of research; see, for example, [2, 5, 7, 12]. These researches often center around fundamental questions: Is it feasible to entirely cover a given region with specific tiles? How many distinct ways can such a region be covered, ensuring that no pair of tiles overlap in their interiors? Can these tilings be linked to other combinatorial objects through bijections, and what inherent combinatorial properties arise from these arrangements?

As researchers focus on larger regions and more intricate tiles, the complexity of these questions intensifies, due to a rapid expansion in the number of possible configurations. Despite these challenges, numerous studies have focused on specific families of regions and tiles, providing insightful answers to these fundamental questions. A classic example involves considering a region as a subset of the plane, with tiles being 1×2 rectangles (commonly known as dominoes or domino tiles), placed on lattice points. The exploration of counting the number of tilings (also called domino tilings) within a given region has garnered significant attention of mathematics. For example, the number of domino tilings of a $m \times n$ rectangle, calculated independently by Kasteleyn [12] and Fisher and Temperley [9], is given by

$$\prod_{j=1}^{\lceil m/2 \rceil} \prod_{k=1}^{\lceil n/2 \rceil} \left(4 \cos^2 \left(\frac{j\pi}{m+1} \right) + 4 \cos^2 \left(\frac{k\pi}{n+1} \right) \right).$$

In particular, using identity (1) from [10], the number of domino tilings for a $2 \times n$ rectangle corresponds to the $(n+1)$ -th Fibonacci number. However, for rectangles with odd dimensions in both width and height (*i.e.*, $(2k+1) \times (2k'+1)$ where k and k' are non-negative integers), the number of domino tilings is zero.

Moreover, researchers have recently employed combinatorial proofs based on tilings to elucidate and extend a diverse range of algebraic identities. Notable instances include connections with the Fibonacci and Pell numbers [13], Hankel determinants [8] and Fibonacci determinants [3]. Elkis, Kuperberg, Larsen and Propp introduced in [7] a compelling family of planar regions, named Aztec diamonds, and extensively studied their tilings with dominoes. The Aztec diamond theorem, a remarkable result in this context, asserts that the number of domino tilings for this specific shape is precisely $2^{n(n+1)/2}$. Furthermore, they developed a methodology that transforms tiling problems into the framework of counting paths on graphs. A concept known as a k -route, representing a set of k non-intersecting lattice paths, becomes instrumental in this approach. Inspired by the work of Gessel and Viennot [11], Eu and Fu established in [8] intriguing connections by associating determinants of *Hankel matrices* (square matrices in which each ascending skew-diagonal from left to right is constant) with the count of k -tuples of non-intersecting large and small Schröder paths. These insightful bijections provide a bridge between the domino tilings of Aztec diamonds and the non-intersecting lattice paths.

An alternative approach to the Aztec diamond theorem appears in [6], where Ciucu derives the recurrence relation $a_n = 2^n a_{n-1}$ by means of perfect matchings of cellular graphs. A *matching* in a graph is a subset of independent edges, *i.e.*, they share no common vertices. This concept has been extensively studied in mathematics and computer science due to its simplicity and wide range of applications, including graph coloring, flow networks, and neural networks. Despite significant research, several open problems remain, such as finding a closed formula for the number of matchings in a graph. In particular, determining the number of perfect matchings, denoted as $m(G)$, in an arbitrary graph G remains an open challenge. While exact closed formulas are elusive, there are asymptotic approximations and exact results for specific graph classes. For instance, considering complete graphs K_n with an even number n of vertices, the number of perfect matchings is given by

$$m(K_n) = \frac{n!}{2^{n/2} \left(\frac{n}{2}\right)!}.$$

Brégman provided in [4] an upper bound for the number of perfect matchings in a balanced bipartite graph in terms of the degrees $d(v)$ of the vertices. Additionally, Kahn and Lovász (unpublished) extended Brégman's bound to an arbitrary graph, yielding the inequality

$$m(G) \leq \prod_{v \in V} (d(v)!)^{1/2d(v)}.$$

On the other hand, in the context of cluster algebras associated to surfaces (an important class of cluster algebras), Musiker, Schiffler, and Williams in [18, 19], obtain a combinatorial formula for the cluster variables whose terms are parameterized by perfect matchings of graphs known as snake graphs. A snake graph \mathcal{G} is a connected planar graph consisting of a finite sequence of square tiles G_1, G_2, \dots, G_d

with $d \geq 1$, such that G_i and G_{i+1} share exactly one edge e_i and this edge is either the north edge of G_i and the south edge of G_{i+1} or the east edge of G_i and the west edge of G_{i+1} , for each $i = 1, \dots, d-1$. Recently, following the ideas of Eu and Fu, I show in [17] how to associate a perfect matching of a ladder graph (or straight snake graph, a graph in which all its tiles lie in one column or one row) to a k -route formed by Schröder paths.

One of the primary objectives of this paper is to construct k -routes associated to perfect matchings of snake graphs from a family of domino tilings over a region constructed from the considered snake graph. Consider a snake graph \mathcal{G} . We define the region $T(\mathcal{G})$, referred to as the snake graph cover, as the union of all unit squares centered at the vertices of \mathcal{G} . Using the domino tilings of $T(\mathcal{G})$, the triangular snake graph $\mathcal{T}_{\mathcal{G}}$ is defined as an acyclic-directed graph with d triangular tiles satisfying specific conditions (see Definition 3.7). Alternatively, employing the well-known operation of edge contraction in graph theory provides an alternative method to construct $\mathcal{T}_{\mathcal{G}}$ (see Definition 3.17). Leveraging Lemma 3.9 and Definition 3.12, the set of k -paths p_i from s_i to t_i , where s_1, \dots, s_k is the set of sources and t_1, \dots, t_k is the set of sinks, can be considered. One may then pose the question: How many of these sets of k paths are k -routes? The following synthesis encapsulates Proposition 3.4, Lemma 3.14, and Theorem 3.21 below, providing an answer to the aforementioned question.

Theorem. Let \mathcal{G} be a snake graph.

- (1) There exists a bijection between the domino tilings of the region $T(\mathcal{G})$ and the set $\text{Match}(\mathcal{G})$ of perfect matchings of \mathcal{G} .
- (2) The set $\text{Match}(\mathcal{G})$ is in bijection with the set of k -routes from s to t in $\mathcal{T}_{\mathcal{G}}$, where $s = (s_1, \dots, s_k)$ and $t = (t_1, \dots, t_k)$.

Çanakçı and Schiffler established in [24] that the number of perfect matchings of \mathcal{G} is equal to the numerator of the continued fraction associated with \mathcal{G} . Consequently, item (1) of the preceding theorem provides insights into determining the count of domino tilings within the region $T(\mathcal{G})$. Furthermore, according to the Lindström-Gessel-Viennot lemma, which asserts that the number of k -routes from s to t in $\mathcal{T}_{\mathcal{G}}$ equals the determinant of the corresponding path matrix M_{st} (as seen in Lemma 2.1), item (2) indicates that this determinant can be regarded as the numerator of the associated continued fraction. Vice versa, the continued fraction associated to \mathcal{G} can be reinterpreted as a quotient of determinants of path matrices.

To establish an explicit connection between snake graphs and Hankel matrices, it is essential to describe how these combinatorial structures intertwine with the study of path matrices and matchings. This exploration reveals a fascinating relationship between the entries of such path matrices and numerical sequences like the Fibonacci sequence and the Catalan numbers.

The Catalan number sequence, denoted by C , is one of the best-known and most important sequences in combinatorics. It has been extensively studied and is associated with over 200 different combinatorial objects, see [22]. This sequence appears in Sloane's On-Line Encyclopedia of Integer Sequences (or OEIS) [20] with the identifier A000108, and is recursively described as follows:

$$C_0 = 1, \quad C_{n+1} = \sum_{i=0}^n C_i C_{n-i}, \quad \text{with } n \geq 0,$$

Additionally, a closed formula for this sequence is given by:

$$C_n = \frac{1}{n+1} \binom{2n}{n}, \quad \text{with } n \geq 0.$$

Examples of objects counted by the Catalan numbers include triangulations of a convex polygon, binary trees, and Dyck paths [21, Corollary 6.2.3].

Similarly, the Fibonacci sequence, denoted by F , is a renowned sequence defined recursively by:

$$F_0 = 0, \quad F_1 = 1, \quad F_{n+1} = F_n + F_{n-1}, \quad \text{for } n > 0.$$

Fibonacci numbers have a wide range of applications in mathematics, computer science, and nature. They appear in various areas, such as the golden ratio, population dynamics, and the structure of plants; see, for example [14].

Our research explores the combinatorial nature of both Catalan and Fibonacci numbers by connecting them to tiling problems and perfect matchings on snake graphs. By extending the concepts of k -routes and perfect matchings, we uncover a deeper relationship between Fibonacci numbers, Catalan numbers, and certain matrix determinants. Recent research has further shown that Hankel matrices can be employed to study these combinatorial sequences. The following synthesis, encompassing Propositions 4.2, 4.4, and 4.7, highlights the connection between Hankel matrices, Catalan numbers, and Fibonacci numbers.

Theorem. Let C be the sequence of Catalan numbers C_n and let F_n be the n -th Fibonacci number. Then the following relationship holds:

$$F_n = \det(H(C)) = \det(M_{st}),$$

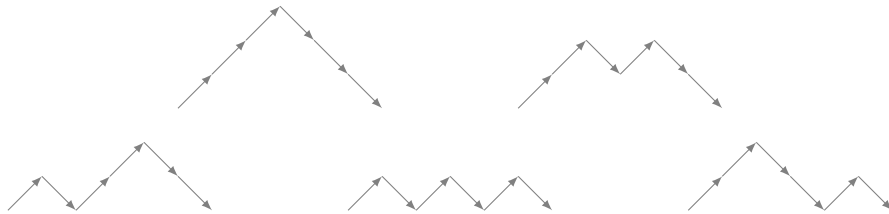
where $H(C)$ is a matrix written in terms of the Hankel matrices of the Catalan numbers, and $M_{st} = (m_{ij})$ is the path matrix associated to the triangular snake graph $\mathcal{T}_{L_{n-2}}$ associated to the vertical ladder graph L_{n-2} .

Additionally, Proposition 4.4 and Proposition 4.7 not only address Hankel matrices with entries from the sequence of Catalan numbers but also provide matrices whose entries are Fibonacci numbers, with determinants matching those of the earlier Hankel matrices. In § 4.2 we explore this property more generally, showing that for snake graphs, the number of perfect matchings can be expressed as a sum of products of Fibonacci numbers, described by the determinant of a matrix with entries given in terms of Fibonacci numbers.

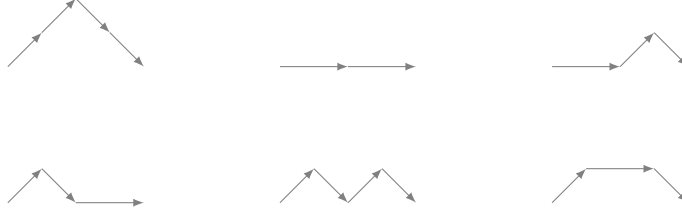
1.2. Organization. The paper is structured as follows. In § 2 we provide the background on lattice paths, Aztec diamonds, Hankel matrices and snake graphs, and set up the notation that will be used throughout the text. In § 3 we give a bijection between non-intersecting lattice paths (or routes) in an acyclic-directed graph and perfect matchings of the snake graph. We also introduce the triangular snake graph \mathcal{T}_G and describe how each perfect matching corresponds to a k -route of \mathcal{T}_G (§ 3.1). Finally, in § 4 we provide key identities in terms of Fibonacci numbers that allow the computation of determinants of matrices, either Hankel matrices associated with Catalan numbers in the case of straight snake graphs, or more generally, determinants of path matrices.

2. BACKGROUND

2.1. Lattice paths and Aztec diamonds. Let S be a subset of \mathbb{Z}^d . A *lattice path* L in \mathbb{Z}^d of length k with steps in S is a sequence $v_0, v_1, \dots, v_k \in \mathbb{Z}^d$ such that each consecutive difference $v_i - v_{i-1}$ belongs to S . L is said to start at v_0 and end at v_k . The enumeration of these paths often leads to interesting numerical sequences. For example, *Dyck paths* (associated to the Catalan numbers) are lattice paths in \mathbb{Z}^2 starting at $(0, 0)$ and ending at $(2n, 0)$ for some $n > 0$, where $S = \{(1, 1), (1, -1)\}$ and the paths do not pass below the x -axis. For fixed n , the set of Dyck paths starting at $(0, 0)$ and ending at $(2n, 0)$ is denoted by \mathcal{D}_n . Notably, the number of elements in \mathcal{D}_n corresponds to the n -th Catalan number. The following 5 lattice paths make up \mathcal{D}_3 .



Another notable example is that of the (large) Schröder number r_n , which count the number of lattice paths from $(0, 0)$ to $(2n, 0)$, for some $n > 0$, using steps from $S = \{(1, 1), (1, -1), (2, 0)\}$ and staying above the x -axis. For a fixed n , let S_n denote the set of these *Schröder paths*. The following 6 lattice paths constitute S_2 .



These numbers are intimately connected to tiling problems. The *Aztec diamond* of order n , denoted by $Az(n)$, is defined as the union of all unit squares whose corners have integer coordinates (x, y) that satisfy $|x| + |y| \leq n + 1$. A *domino tile* is a rectangle of size 1 by 2 or 2 by 1 with corners with integer coordinates. A *domino tiling* of $Az(n)$ is a set of non-overlapping dominoes whose union is $Az(n)$. In [7], it was first proven that the number of domino tilings for the Aztec diamond $Az(n)$ is $2^{n(n+1)/2}$. This significant outcome, commonly referred to as the Aztec Diamond Theorem, has been proved in different ways. One such proof was presented by Eu and Fu in [8] using Hankel determinants of the large and small Schröder numbers. This proof relies on a bijection connecting domino tilings of an Aztec diamond to non-intersecting lattice paths. The essential idea behind this bijection involves labeling the rows of $Az(n)$ with numbers from 1 to $2n$ (from bottom to top). For each $1 \leq i \leq n$, a path p_i is defined, starting from the center of the left edge of the i -th row and ending at the center of the right edge of the same row. Whenever the path reaches a high domino, it traverses through the domino, switching from top to bottom or vice versa. For wide dominoes, the path moves horizontally. The dominoes above the highest path are exclusively wide. Therefore, to establish a correspondence between Aztec diamonds and Schröder paths, specific decorated dominoes are introduced. Each domino is depicted as follows:



2.2. Hankel matrices and lattice paths. A well-known problem in linear algebra is the study of *Hankel matrices*, which are $n \times n$ matrices $B = (b_{ij})$ such that, for $i \leq j$, we have $b_{ij} = b_{i+k, j-k}$, for all $k \in [j - i]$. In combinatorics specifically, we study Hankel matrices associated with a sequence $\mathcal{B} = \{b_n\}_{n \in \mathbb{N}}$, which are defined in [1, p.53] as

$$H_n(\mathcal{B}) = \begin{pmatrix} b_0 & b_1 & \cdots & b_{n-1} \\ b_1 & b_2 & \cdots & b_n \\ \vdots & \vdots & \ddots & \vdots \\ b_{n-1} & b_n & \cdots & b_{2n-2} \end{pmatrix} \quad \text{and} \quad H'_n(\mathcal{B}) = \begin{pmatrix} b_1 & b_2 & \cdots & b_n \\ b_2 & b_3 & \cdots & b_{n+1} \\ \vdots & \vdots & \ddots & \vdots \\ b_n & b_{n+1} & \cdots & b_{2n-1} \end{pmatrix}.$$

In particular, the *Hankel determinant* of order n of \mathcal{B} (sometimes called the *Hankel transform*), is the determinant of the corresponding Hankel matrix of order n . The Hankel determinant was first introduced in OEIS with Sloane's sequence A055878 and later studied by Layman [15]. Many interesting properties of Hankel determinants are known. For instance, for the Catalan sequence, we obtain that

$$\det H'_n(C) = \begin{vmatrix} C_1 & C_2 & \cdots & C_n \\ C_2 & C_3 & \cdots & C_{n+1} \\ \vdots & \vdots & \ddots & \vdots \\ C_n & C_{n+1} & \cdots & C_{2n-1} \end{vmatrix} = 1.$$

To find some properties for the determinants of the Hankel matrices associated with the sequence of Catalan numbers we can use the Lindström-Gessel-Viennot lemma. To state this lemma, we first introduce the concepts of routes and path matrices. Let $G = (V, E)$ be a directed graph and let $n \in \mathbb{N}$. A n -vertex $s = (s_1, \dots, s_n)$ of G is an n -tuple where $s_i \in V$, for all $i \in [n]$. If $s = (s_1, \dots, s_n)$ and $t = (t_1, \dots, t_n)$ are n -vertices of G , define a n -path (also called *path system*) $P = (p_1, \dots, p_n)$ from s to t , where p_i is a path from s_i to t_i .

If the paths p_i and p_j do not have vertices in common, for $1 \leq i, j \leq n$, they are *vertex-disjoint paths*. The n -path $R = (p_1, \dots, p_n)$ is a n -route if p_i and p_j are vertex-disjoint, for all $i \neq j$. Let A be a commutative ring and let $w : E \rightarrow A$ be a weight function on the edges of a directed graph G .

The *weight* of a n -route R , denoted as $w(R)$, is the product of the weights of the edges in the paths:

$$w(R) = \prod_{i=1}^n \prod_{e \in p_i} w(e).$$

The *path matrix* $M_{st} = (m_{ij})_{1 \leq i, j \leq n}$ between two n -vertices $s = (s_1, \dots, s_n)$ and $t = (t_1, \dots, t_n)$ is defined as follows:

$$m_{ij} = \sum_{p: s_i \rightarrow t_j} w(p).$$

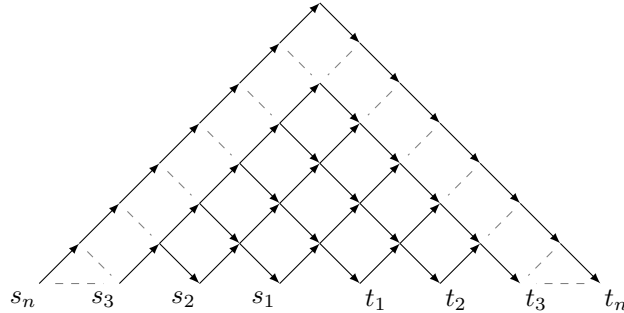
In particular, if $w(e) = 1$ for all edges $e \in E$ (unweighted graph), the path matrix $M_{st} = (m_{ij})_{1 \leq i, j \leq n}$ from $s = (s_1, \dots, s_n)$ to $t = (t_1, \dots, t_n)$ is such that m_{ij} is equal to the number of paths from s_i to t_j .

Lemma 2.1 (Lindström [16], Gessel-Viennot [11, Theorem 1]). Let G be an acyclic directed unweighted graph, and let $s = (s_1, \dots, s_n)$ and $t = (t_1, \dots, t_n)$ be two n -vectors of G , then

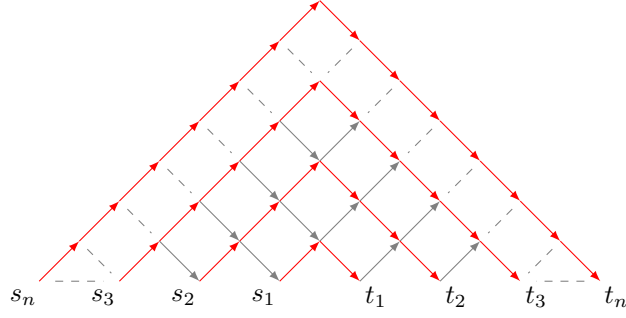
$$\det M_{st} = |\{R : R \text{ is a } n\text{-route from } s \text{ to } t\}|,$$

where M_{st} is the path matrix between s and t .

An example relating the previous concepts is given by the graph below with n -vertices $s = (s_1, \dots, s_n)$ and $t = (t_1, \dots, t_n)$



According to the picture, the paths from s_i to t_k are Dyck paths, in this way, the path matrix is $M_{st} = (m_{ij})$, where $m_{ij} = C_{i+j-1}$, which is the Hankel matrix $H'_n(C)$ associated to the sequence C of Catalan numbers. Additionally, only the n -route is the following

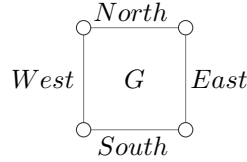


Therefore, using the Lemma 2.1, we conclude that $\det H'_n(C) = 1$.

2.3. Perfect matchings and snake graphs. In [23] and [24] the authors introduced a useful relationship between the continued fraction associated with a snake graph, the number of perfect matchings of such graph and a cluster algebra. These relationships became a tool to simplify some problems associated with each of these objects, and they are one of the main interest of the present work.

Let $G = (V, E)$ be a graph with $|V| = n$ and let $S \subset E$. The set S is said to be a *matching* on G , if these edges do not have vertices in common. If each vertex in G is incident to an edge of S , then S is a *perfect matching* and $|S| = \frac{n}{2}$. We denote by $\text{Match}(G)$ the set of perfect matchings of G .

We consider a tile G as a graph that has the following form:



A *snake graph* \mathcal{G} is a connected planar graph consisting of a finite sequence of tiles G_1, G_2, \dots, G_d , with $d \geq 1$, in such a way that for each $i \in [d-1]$, the G_i and G_{i+1} tiles share exactly one edge e_i , which is the North edge of G_i and the South edge of G_{i+1} , or the East edge of G_i and the West edge of G_{i+1} . The edges e_i that are contained in two tiles are called *interior edges*. For a snake graph made up of tiles G_1, G_2, \dots, G_d , the interior edges are e_1, e_2, \dots, e_{d-1} . All of the other edges are called *boundary edges*.

The edges of a graph can be assigned the symbols $+$ or $-$, giving rise to a sign function f on a snake graph \mathcal{G} which is an application $f : E(\mathcal{G}) \rightarrow \{+, -\}$ such that for each tile G_i in \mathcal{G} the following conditions are met:

- The north and west edges of G_i have the same sign,
- The south and east edges of G_i have the same sign,
- The sign of the north edge is opposite to the sign of the south edge.

Additionally, a continued fraction can be associated to a snake graph by means of its sign function as follows: If \mathcal{G} is a snake graph with d tiles, then the sequence of signs

$$[f(e_0), f(e_1), \dots, f(e_{d-1}), f(e_d)],$$

where e_1, \dots, e_{d-1} are the interior edges of \mathcal{G} , e_0 is the south edge of G_1 and e_d is the north edge of G_d . If $\epsilon \in \{+, -\}$ we have

$$(2.1) \quad [f(e_0), f(e_1), \dots, f(e_{d-1}), f(e_d)] = [\underbrace{\epsilon, \dots, \epsilon}_{a_1}, \underbrace{-\epsilon, \dots, -\epsilon}_{a_2}, \dots, \underbrace{\pm\epsilon, \dots, \pm\epsilon}_{a_n}],$$

then the continued fraction $[a_1, \dots, a_n]$ associated with \mathcal{G} is obtained, where

$$[a_1, \dots, a_n] = a_1 + \frac{1}{a_2 + \frac{1}{a_3 + \frac{1}{\ddots + \frac{1}{a_n}}}}.$$

Now let $[a_1, \dots, a_n]$ be a positive continued fraction (*i.e.*, if each $a_i \in \mathbb{Z}_{>0}$). The snake graph associated to the continued fraction $[a_1, \dots, a_n]$ is denoted by $\mathcal{G}[a_1, \dots, a_n]$ and is the snake graph with $d = a_1 + a_2 + \dots + a_n - 1$ tiles determined by the sign sequence 2.1. The following theorem relates the continued fractions of a snake graph with its perfect matchings.

Theorem 2.2 ([24]). If $m(\mathcal{G})$ denotes the number of perfect matchings of \mathcal{G} then

$$[a_1, a_2, \dots, a_n] = \frac{m(\mathcal{G}[a_1, a_2, \dots, a_n])}{m(\mathcal{G}[a_2, \dots, a_n])}.$$

As an application of Theorem 2.2, we note that the numerator of the continued fraction of $[a_1, \dots, a_n]$ corresponds to the number of perfect matchings in the snake graph $\mathcal{G}[a_1, \dots, a_n]$. Similarly, the numerator of $[a_n, \dots, a_1]$ represents the number of perfect matchings in $\mathcal{G}[a_n, \dots, a_1]$. Since these two snake graphs are identical up to a 180-degree rotation, they must have the same number of perfect matchings. This leads to the following result.

Theorem 2.3 ([24]). The continued fractions $[a_1, \dots, a_n]$ and $[a_n, \dots, a_1]$ have the same numerator.

Observe that if $[a_1, \dots, a_n]$ is a continued fraction with $a_n = 1$, then $[a_1, \dots, a_n] = [a_1, \dots, a_{n-1} + 1]$. This property, along with Theorem 2.3, will be used in § 4.2.

3. PERFECT MATCHINGS, TILINGS AND NON-INTERSECTING LATTICE PATHS

In this section, we will construct an acyclic directed graph corresponding to each snake graph. This construction will establish a bijection between the routes (non-intersecting lattice paths) in the resulting acyclic-directed graph and the perfect matchings of the snake graph. This construction was motivated by the bijection between domino tilings of an Aztec diamond and non-intersecting lattice paths (large Schröder paths satisfying some particular conditions) given by Eu and Fu in [8].

3.1. Tilings and snake graphs. Without loss of generality and for an easier exposition, let us consider a snake graph \mathcal{G} formed by a sequence of unit squares G_1, G_2, \dots, G_d , where $d \geq 1$.

Definition 3.1. The *cover* $T(G_i)$ of tile G_i in a snake graph \mathcal{G} is the union of all unit squares centered at the vertices of G_i . The *snake graph cover* $T(\mathcal{G})$ of a snake graph \mathcal{G} is the union of the covers of all tiles G_i in \mathcal{G} .

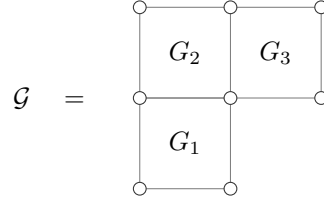


FIGURE 1. From left to right, tile G_i of a snake graph \mathcal{G} and its cover $T(G_i)$.

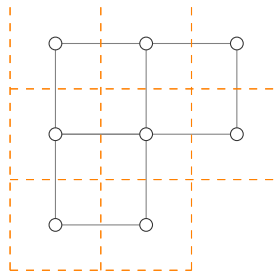
The unit square centered at the southwest vertex of the tile G_1 is called the *initial tile* of $T(\mathcal{G})$.

Definition 3.2. A *domino tile* is formed by the union of any two unit squares sharing an edge. A *snake graph tiling* of \mathcal{G} is a set of non-overlapping domino tiles whose union forms $T(\mathcal{G})$. We denote the set of all snake graph tilings of \mathcal{G} by $\text{Til}(\mathcal{G})$.

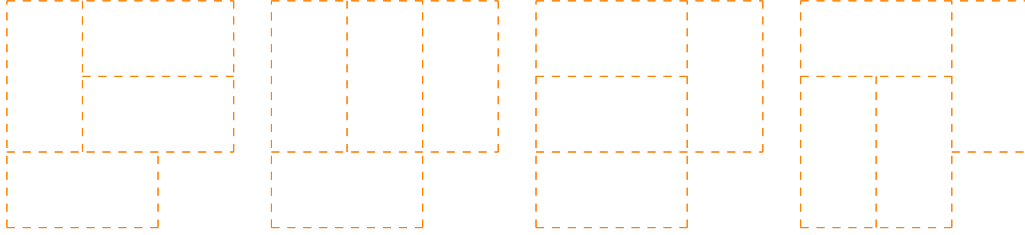
Example 3.3. Consider the snake graph



The snake graph cover $T(\mathcal{G})$ corresponding to it is



There exist precisely four snake graph tilings of \mathcal{G}



Proposition 3.4. Let \mathcal{G} be a snake graph. There exists a bijection between the set $\text{Til}(\mathcal{G})$ of snake graph tilings of \mathcal{G} and the set $\text{Match}(\mathcal{G})$ of perfect matchings of \mathcal{G} .

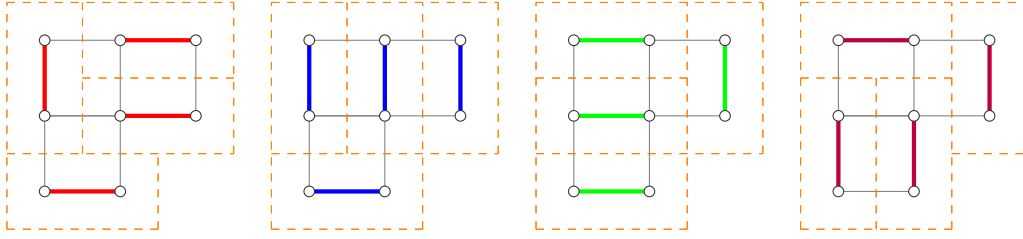
Proof. Given $P \in \text{Match}(\mathcal{G})$, we associate a snake graph tiling as follows: For an edge e_{ij} in P connecting the vertices v_i and v_j in \mathcal{G} , we create a domino tile D_{ij} associated to e_{ij} by linking the unit squares centered at v_i and v_j . If two distinct edges e_{ij} and e_{kl} exist in P , the intersection of the domino tiles D_{ij} and D_{kl} is empty. Otherwise, the existence of a common vertex between e_{ij} and e_{kl} would contradict the assumption of P being a matching of \mathcal{G} . Moreover,

$$\bigcup_{e_{ij}} D_{ij} = T(\mathcal{G}),$$

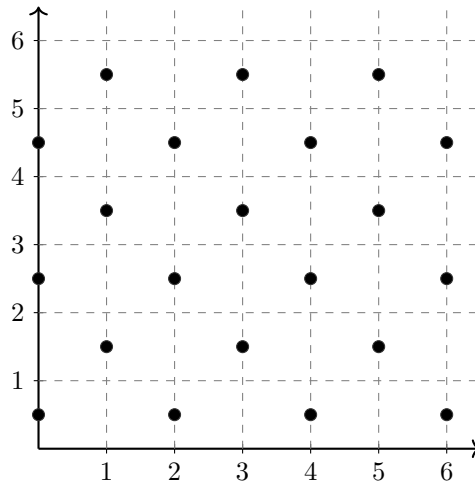
where the union is taken over all edges e_{ij} in P . This holds because for each edge e_{kl} in P , there exists a tile G_i in \mathcal{G} such that e_{kl} is an edge of G_i , and thus $D_{kl} \subset T(G_i) \subset T(\mathcal{G})$. Furthermore, as P is a perfect matching, for each cover $T(G_i)$ there exist edges e_{pq} in P such that $T(G_i) \subseteq \bigcup_{e_{pq}} D_{pq}$. Conversely, considering a snake graph tiling of \mathcal{G} , for every vertex v_p of \mathcal{G} , there exists a unique domino tile such that v_p is the center of one of the unit squares contained in that domino tile. Let v_q be the center of the other unit square. We construct a perfect matching P where the edge e_{pq} from v_p to v_q is an edge of P .

This proves the bijection between snake graph tilings and perfect matchings in \mathcal{G} . \square

Example 3.5. Let \mathcal{G} the snake graph in the Example 3.3. Then, the perfect matchings associated to the four snake graph tilings are



3.2. Decorated snake graph tilings and paths. We intend to establish a correspondence between routes and snake graph tilings. To achieve this, we define a grid in $(\mathbb{R}_{\geq 0})^2$, placing black points at coordinates $(2n, 2m + 0.5)$ and $(2n + 1, 2m + 1.5)$, where n and m are elements of \mathbb{N} .



Subsequently, we position the snake graph cover $T(\mathcal{G})$ of \mathcal{G} on the grid, ensuring that the southwest vertex of the initial tile of $T(\mathcal{G})$ aligns with $(0, 0)$, thus establishing a decoration using black points within the snake graph cover. We can observe that the snake graph cover is decorated with the following two unit squares

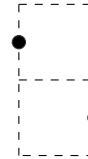
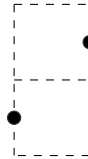
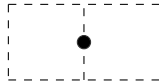
Right-decorated square



Left-decorated square



in such a way that the initial tile of $T(\mathcal{G})$ is left-decorated, and each square that shares an edge with a left-decorated square is right-decorated, and vice versa. In this way, any domino tile in a snake graph tiling will be decorated in one of the following ways



So decorated dominoes can be naturally associated to these figures as follows:

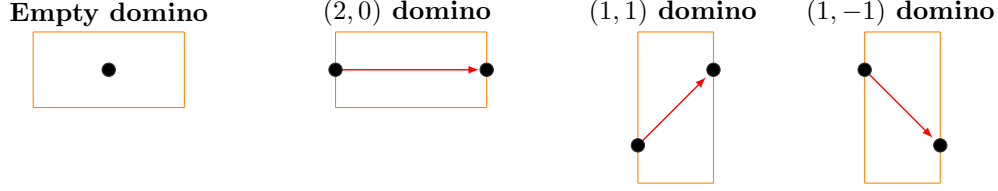
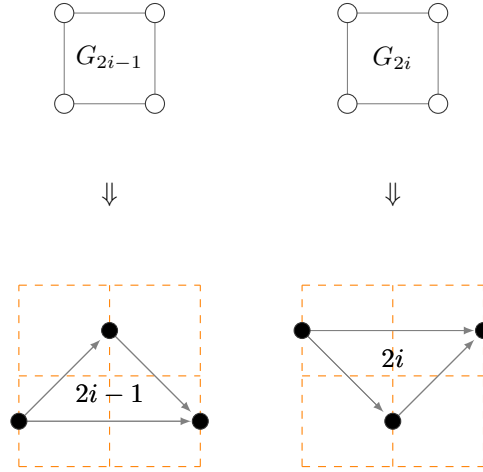


FIGURE 2. Decorated dominoes.

Remark 3.6. While the coordinates of the black points in the grid are not aligned with integers on the y -axis, a simple translation by 0.5 units downwards shows that the resulting grid does indeed possess integer coordinates. Based on this observation, we classify each of the paths derived from the decorated snake graph tilings as a lattice path with steps $S = \{(2, 0), (1, 1), (1, -1)\}$.

Definition 3.7. The *triangular snake graph* $\mathcal{T}_{\mathcal{G}}$ associated to \mathcal{G} is a connected acyclic-directed graph derived from the decorated snake graph cover. It is constructed by placing an arrow between two distinct black points if the corresponding unit squares share an edge as shown in Figure 2.

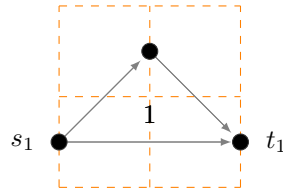
Remark 3.8. Notably, the black points that belong to only one square in $T(\mathcal{G})$ are sources or sinks. Considering that the arrows in the triangular snake graph are oriented from left to right, the sources (resp. the sinks) reside on a domino tile's left-hand side (resp. right-hand side). Additionally, note that every tile G_j of \mathcal{G} contributes a triangular tile labeled by the number j , depending on the parity of j , as follows:



We will now prove some other not-so-obvious properties about $\mathcal{T}_{\mathcal{G}}$.

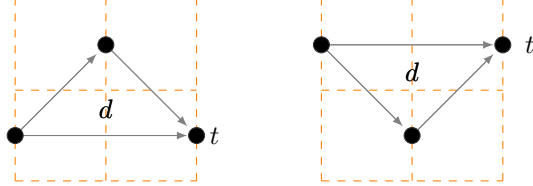
Lemma 3.9. Let $\mathcal{T}_{\mathcal{G}}$ be the triangular snake graph associated to \mathcal{G} . Then $\mathcal{T}_{\mathcal{G}}$ possesses an equal number of sources and sinks.

Proof. The proof proceeds by induction on the number of tiles in \mathcal{G} . For the base case when $d = 1$, $\mathcal{G} = G_1$, then the triangular snake graph $\mathcal{T}_{\mathcal{G}}$ associated to G_1 is depicted as:



In this case, there exists one source s_1 and one sink t_1 . Assume the statement holds true for any snake graph with d tiles, $d > 1$. We will now establish its validity for a snake graph \mathcal{G}_{d+1} containing $d + 1$ tiles.

Consider the snake graph \mathcal{G}_d obtained by removing the last tile G_{d+1} from \mathcal{G}_{d+1} . By the induction hypothesis, $\mathcal{T}_{\mathcal{G}_d}$ has an equal number of sources and sinks. Now, we examine two possible scenarios for the last part of the triangular snake graph of \mathcal{G}_d :



If tiles G_d and G_{d+1} share the edge e_d , where e_d is the north edge of G_d and the south edge of G_{d+1} , we obtain two possible different structures:

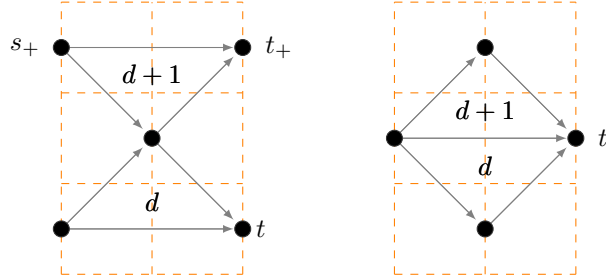


FIGURE 3. Triangular tiles associated to the tiles G_d and G_{d+1} that share the north and south edge.

In the first case, the resulting triangular snake graph of \mathcal{G}_{d+1} encompasses all the sources and sinks of \mathcal{G}_d . Additionally, two new elements are introduced: a source s_+ and a sink t_+ as depicted in the left of Figure 3. Conversely, in the second case, the sources and sinks in both \mathcal{G}_d and \mathcal{G}_{d+1} are equal. This distinction arises due to the structural differences between the configurations of adjoining tiles.

On the other hand, if the tiles G_d and G_{d+1} share the edge e_d , where e_d is the east edge of G_d and the west edge of G_{d+1} , we obtain one of the following scenarios

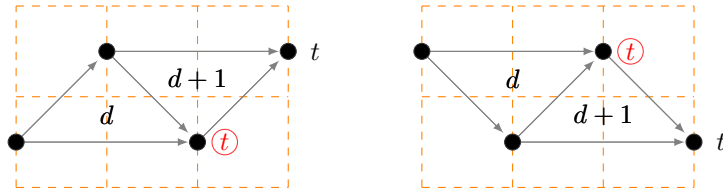


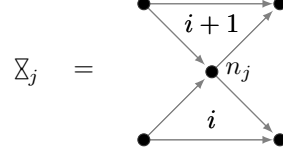
FIGURE 4. Triangular tiles associated to the tiles G_d and G_{d+1} that share the east and west edge.

Upon close examination, it becomes evident that the element identified as the sink t in \mathcal{G}_d is no longer a sink of $\mathcal{T}_{\mathcal{G}_{d+1}}$. Instead, the southeast black point within the new triangular tile takes over the role previously attributed to the mentioned sink.

In either case, the count of sources and sinks remains equal, thereby completing the proof. \square

The proof of Lemma 3.9 yields an additional insight: the number of sources and sinks increases with the appearance of a specific subgraph within the triangular snake graph. This subgraph is formally defined in the following definition.

Definition 3.10. An *hourglass graph* is a graph with the following structure:



The vertex n_j will be called the *neck* of the hourglass graph \mathbb{X}_j . The triangular subgraphs labeled by $i+1$ and i are the *head* and *body* of \mathbb{X}_j , respectively.

As a direct consequence, we establish the following corollary.

Corollary 3.11. Let $\mathcal{T}_{\mathcal{G}}$ be the triangular snake graph associated to \mathcal{G} . $\mathcal{T}_{\mathcal{G}}$ contains $k-1$ hourglass graphs as subgraphs if and only if the number of sources (and sinks) in $\mathcal{T}_{\mathcal{G}}$ is k , where $k \geq 1$.

Proof. The proof follows a similar structure as the proof of Lemma 3.9 and will only be indicated briefly. We proceed by induction based on the number of sources in $\mathcal{T}_{\mathcal{G}}$. For the base case, when $\mathcal{T}_{\mathcal{G}}$ has no hourglass graphs, the number of sources (and sinks) is 1. When $\mathcal{T}_{\mathcal{G}}$ has only one hourglass graph, the number of sources (and sinks) is 2. Assuming the validity of the statement for any triangular snake graph with $k-1$ hourglasses, we aim to establish its validity for a triangular snake graph $\mathcal{T}_{\mathcal{G}}$ containing k hourglasses.

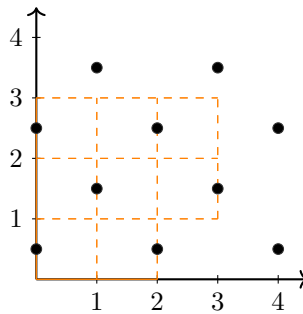
Let us consider the triangular snake graph $\mathcal{T}_{\mathcal{G}}^-$ obtained by removing the triangular tiles labeled by i from $\mathcal{T}_{\mathcal{G}}$, for $i > j$, where j is the label of the body of the last hourglass \mathbb{X}_k . Then, $\mathcal{T}_{\mathcal{G}}^-$ contains $k-1$ hourglass graphs. According to the induction hypothesis, $\mathcal{T}_{\mathcal{G}}^-$ possesses k sources (and sinks). A similar analysis to that in the proof of Lemma 3.9, shows that $\mathcal{T}_{\mathcal{G}}$ has $k+1$ sources (and sinks). To prove the reverse implication, assume $\mathcal{T}_{\mathcal{G}}$ contains k sources (and sinks). By induction on the number of sources, the same reasoning can be applied to show that $\mathcal{T}_{\mathcal{G}}$ contains $k-1$ hourglass graphs as subgraphs. \square

Unless stated otherwise, we assume that $\mathcal{T}_{\mathcal{G}}$ possesses k sources, denoted as s_1, s_2, \dots, s_k , and k sinks, denoted as t_1, t_2, \dots, t_k . To describe the k -routes of $\mathcal{T}_{\mathcal{G}}$, these k -vertices of $\mathcal{T}_{\mathcal{G}}$ are defined as follows.

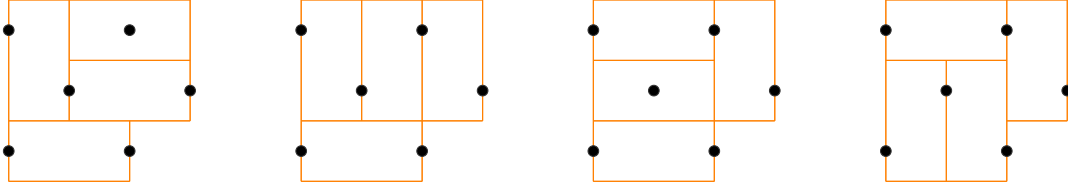
Definition 3.12. The k -vertices $s = (s_1, \dots, s_k)$ and $t = (t_1, \dots, t_k)$ of $\mathcal{T}_{\mathcal{G}}$ are defined by imposing the following conditions:

- (1) $\mathcal{T}_{\mathcal{G}}$ contains $k-1$ hourglass graphs as subgraphs.
- (2) $s = (s_1, \dots, s_k)$ and $t = (t_1, \dots, t_k)$ are ordered vectors formed by the sources and sinks in $\mathcal{T}_{\mathcal{G}}$, respectively.
- (3) If s_i and s_j (respectively t_i and t_j) are vertices such that $i < j$, then the y-coordinate of s_i (respectively t_i) is less than the y-coordinate of s_j (respectively t_j).

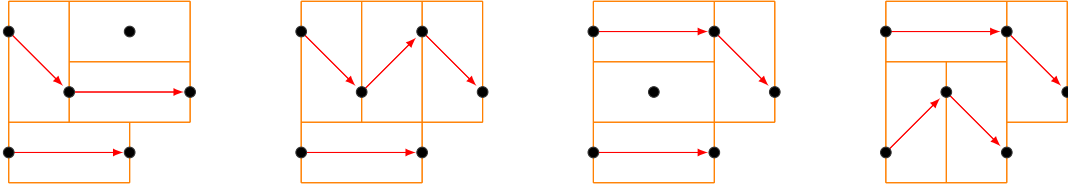
Example 3.13. Let \mathcal{G} the snake graph in the Example 3.3. The snake graph cover on the grid is depicted as follows:



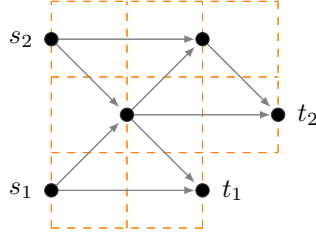
The snake graph tilings are



Then, we obtain the following decorated snake graph tilings associated to perfect matchings depicted in Example 3.5



and the triangular snake graph $\mathcal{T}_{\mathcal{G}}$ with its 2-vertices, $s = (s_1, s_2)$ and $t = (t_1, t_2)$, is



We can observe that each decorated snake graph tiling contains two paths that do not intersect. Additionally, the paths start at vertex s_i and end at vertex t_i , for some $i \in \{1, 2\}$.

Lemma 3.14. Let $P \in \text{Match}(\mathcal{G})$. Then the decorated snake graph cover associated to P represents a k -route from s to t in $\mathcal{T}_{\mathcal{G}}$.

Proof. Let $p = (v_{l+1}|\alpha_l, \alpha_{l-1}, \dots, \alpha_1|v_1)$ be a maximal path in the decorated snake graph tiling associated to $P \in \text{Match}(\mathcal{G})$ such that p starts at vertex v_1 and ends at vertex v_{l+1} . There exist l decorated domino tiles with steps $(2, 0)$, $(1, 1)$ or $(1, -1)$ in such a way that every arrow α_i of p corresponds to one of these decorated domino tiles. We claim that v_1 is a source and v_{l+1} is a sink in $\mathcal{T}_{\mathcal{G}}$. Otherwise, if v_1 is not a source, then it would be on the right-hand side of a domino tile D_{v_1} , leading to two possible cases:

- (1) D_{v_1} is an empty domino. This case contradicts the requirement that consecutive horizontal black points should maintain a distance of 2 units, not one.
- (2) D_{v_1} is a $(2, 0)$, $(1, 1)$, or $(1, -1)$ domino. This case breaches the requirement that p is a maximal path starting at v_1 in the decorated snake graph tiling associated to P .

Similarly, if v_{l+1} is not a sink, it would be on the left-hand side of a domino tile $D_{v_{l+1}}$, and the same two cases apply as for v_1 . Consequently, there must exist $i, j \in [k]$ such that $v_1 = s_i$ and $v_{l+1} = t_j$.

It is now necessary to prove that indeed $i = j$. Suppose $i \neq j$. Then, p traverses an hourglass graph in one of the three ways shown on the left of Figure 5.

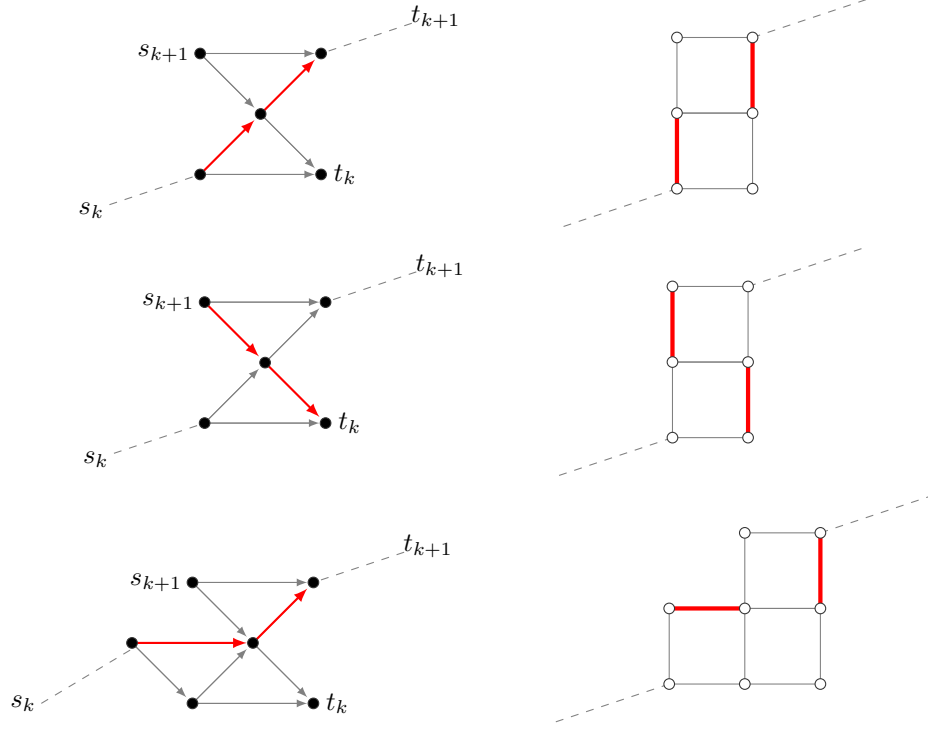


FIGURE 5. The 3 cases in which p is a path starting at s_i and ending at t_j , $i \neq j$.

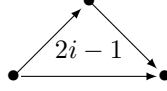
If any of these cases were to occur, the perfect matching P would have the edge configurations illustrated in one of the three cases on the right side of Figure 5. However, by parity considerations, this situation is not possible, as both the right and left sides of P would inevitably contain at least one unmatched vertex. Consequently, none of these cases results in a valid perfect matching, affirming that any path p in the decorated snake graph tiling associated to a perfect matching P starts at a source s_i and ends at a sink t_i .

Moreover, consider two paths p and p' where p starts at s_i and ends at t_i , while p' starts at s_j and ends at t_j . If $s_i \neq s_j$ and $t_i \neq t_j$, their intersection at a vertex v implies the existence of α and α' on p and p' , respectively, such that v is a common vertex of both arrows. This contradicts the requirement that the domino tiles containing α and α' must be non-overlapping, as imposed by the snake graph tiling.

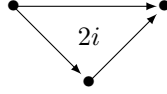
Hence, we have proved that the paths in the snake graph tiling are paths exclusively from s_i to t_i , for $i \in [k]$, and these paths are vertex-disjoint. Therefore, each perfect matching provides a unique k -route from s to t in \mathcal{T}_G , thereby completing the proof. \square

Remark 3.15. It is evident that if we consider two distinct perfect matchings, their respective k -routes will differ. Specifically, if e is an edge present in the perfect matching P but absent in the perfect matching P' , then the k -route R_P will contain a decorated domino (either an empty, $(2, 0)$, $(1, 1)$ or a $(1, -1)$ domino) that is not present in $R_{P'}$. In the cases where the domino in R_P that is absent in $R_{P'}$ is a $(2, 0)$, $(1, -1)$, or $(1, 1)$ domino, then the corresponding arrow will be absent in $R_{P'}$. In the case where the empty edge formed by squares centered on the vertices v_1 and v_2 (where they are right-decorated and left-decorated squares, respectively) is present in R_P , we observe that in $R_{P'}$ there exist two dominoes $((2, 0), (1, 1)$ or a $(1, -1))$ D_1 and D_2 , in such a way that the square centered at v_1 is in D_1 , and the square centered at v_2 is in D_2 . Consequently, the arrows corresponding to D_1 and D_2 are present in $R_{P'}$ but absent in R_P .

3.3. Edge contraction in snake graphs. Now, we are going to consider Remark 3.8. Again we consider a snake graph \mathcal{G} , which is built by the sequence of tiles G_1, G_2, \dots, G_d , with $d \geq 1$. If d is an even number (resp. an odd number), then tiles G_{2i-1} , with $i \in \{1, 2, \dots, \lfloor d/2 \rfloor\}$ (resp. $i \in \{1, 2, \dots, \lfloor d/2 \rfloor + 1\}$) will be identified with the subgraph



and the tiles G_{2i} , with $i \in \{1, 2, \dots, \lfloor d/2 \rfloor\}$ will be identified with the subgraph

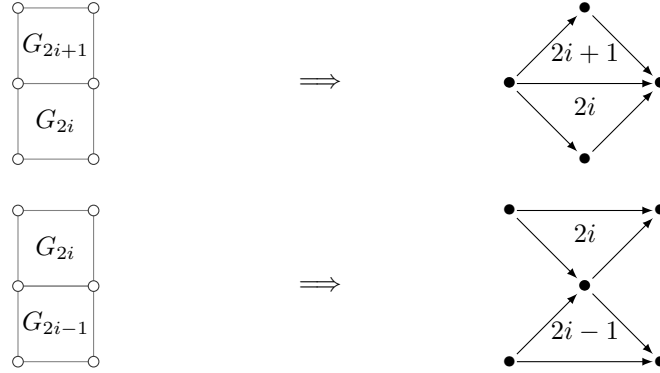


Then the acyclic-directed graph $\mathcal{T}_{\mathcal{G}}$ is formed by the following rules:

- (1) If the tiles G_j and G_{j+1} of the snake graph \mathcal{G} are joined by their east and west sides, then the respective triangles labeled by j and $j+1$ are joined by the arrows corresponding to the steps $(1, 1)$ and $(1, -1)$ as follows:

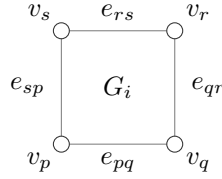


- (2) If the tiles G_j and G_{j+1} of the snake graph \mathcal{G} are joined by their north and south sides, then the respective triangles labeled by j and $j+1$ are joined by their north and south arrows (corresponding to steps $(1, 0)$) or by their north and south vertices, as follows:



We can see that the construction of $\mathcal{T}_{\mathcal{G}}$ is very similar to that of \mathcal{G} , except for the shape of the tiles (the square tiles are changed to triangular tiles). Therefore, making use of the operation in graph theory called edge contraction, and thinking about maintaining the information alluding to the cluster variables seen in § 2.3, we are going to make a different construction than the one introduced in § 3.1.

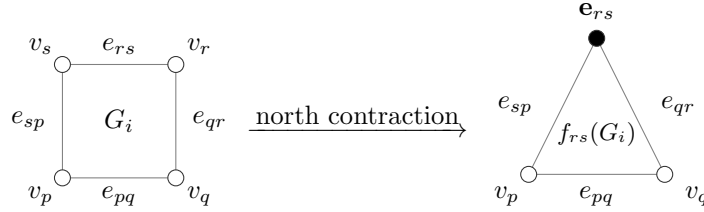
Definition 3.16. Let \mathcal{G} a snake graph and let $G_i = (V_i, E_i)$ a tile of \mathcal{G} , where $V_i = \{v_p, v_q, v_r, v_s\}$ and $E_i = \{e_{pq}, e_{qr}, e_{rs}, e_{sp}\}$:



Let f_{rs} be a function that maps every vertex in $V_i - \{v_r, v_s\}$ to itself, and otherwise maps v_r and v_s to a new vertex \mathbf{e}_{rs} . We define the *north contraction* of G_i as a new graph $f_{rs}(G_i) = (\hat{V}_i, \hat{E}_i)$, where

$$\hat{V}_i = (V_i - \{v_r, v_s\}) \cup \{\mathbf{e}_{rs}\} \quad \text{and} \quad \hat{E}_i = E_i - \{e_{rs}\},$$

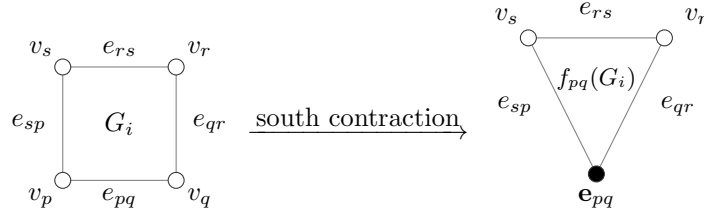
and for every $v \in V_i$, we have that $f_{rs}(v) \in \hat{V}_i$ is incident to an edge $e \in \hat{E}_i \subset E_i$ if and only if e is incident to v in G_i .



Analogously, let f_{pq} be a function that maps every vertex in $V_i - \{v_p, v_q\}$ to itself, and otherwise, maps v_p and v_q to a new vertex \mathbf{e}_{pq} . We define the *south contraction* of G_i as a new graph $f_{pq}(G_i) = (\check{V}_i, \check{E}_i)$, where

$$\check{V}_i = (V_i - \{v_p, v_q\}) \cup \{\mathbf{e}_{pq}\} \quad \text{and} \quad \check{E}_i = E_i - \{e_{pq}\},$$

and for every $v \in V_i$, we have that $f_{pq}(v) \in \check{V}_i$ is incident to an edge $e \in \check{E}_i \subset E_i$ if and only if e is incident to v in G_i .



If no confusion arises, any north contraction (resp. south contraction) will be simply called f_N (resp. f_S).

Definition 3.17. Let \mathcal{G} be a snake graph with d tiles and interior edges e_1, e_2, \dots, e_{d-1} . The *contracted snake graph* associated to \mathcal{G} is a connected planar graph consisting of a finite sequence of tiles T_1, T_2, \dots, T_d in such a way that

- (1) $T_i = f_N(G_i)$ if i is odd, and otherwise, $T_i = f_S(G_i)$ if i is even.
- (2) For each $i \in [d-1]$, T_i and T_{i+1} share exactly the edge e_i or the vertex \mathbf{e}_i .

The *oriented contracted snake graph* is obtained when we put orientations to the edges of the contracted snake graph with the condition that the arrows are oriented from left to right.

Remark 3.18. In order to generate equivalent lattice paths in the oriented contracted snake graph, as discussed in § 3.1 for $\mathcal{T}_{\mathcal{G}}$ and characterized by steps from the set $\{(2, 0), (1, 1), (1, -1)\}$, we can consider an isomorphic snake graph to \mathcal{G} in Definition 3.17 with tiles G_i as 1×2 rectangles. Consequently, the oriented contracted snake graph of \mathcal{G} is canonically isomorphic to the triangular snake graph $\mathcal{T}_{\mathcal{G}}$. Therefore, we systematically identify these graphs. Hence we can think of $\mathcal{T}_{\mathcal{G}}$ either as a triangular snake graph or as an oriented contracted snake graph. The k -vertices $s = (s_1, \dots, s_k)$ and $t = (t_1, \dots, t_k)$ (as defined in Definition 3.12) are also considered within this context.

Lemma 3.19. Let $\mathcal{T}_{\mathcal{G}}$ be the oriented contracted snake graph of \mathcal{G} . The sinks and sources are the only vertices that are not the result of contractions of edges of \mathcal{G} .

Proof. This directly follows from Definition 3.16. If \mathbf{e}_{pq} represents the contraction of the edge e_{pq} within a tile G_i of \mathcal{G} , then the west and east edges of G_i are incident to \mathbf{e}_{pq} , with the west arrow directed into \mathbf{e}_{pq} and the east arrow directed out of \mathbf{e}_{pq} . Consequently, the vertices obtained through edge contractions cannot serve as sources or sinks. Moreover, any other vertex is obtained by an edge contraction as it is either the top or the bottom of a triangular tile. \square

Remark 3.20. A *decontraction* process can be applied to $\mathcal{T}_{\mathcal{G}}$ to reconstruct the snake graph \mathcal{G} from $\mathcal{T}_{\mathcal{G}}$. According to Lemma 3.19, the sources, sinks, and their incident arrows remain unchanged. However, for each vertex \mathbf{e} in $\mathcal{T}_{\mathcal{G}}$ that is neither a source nor a sink, two new vertices, v_e and v'_e , along with the edge e , are introduced. The arrows that end at \mathbf{e} become incident to the vertex v_e , while those that start at \mathbf{e} will be incident to the vertex v'_e . Formally, this process is defined as follows: Let $\mathcal{T}_{\mathcal{G}} = (\overline{V}, \overline{E})$ be the oriented contracted snake graph associated to \mathcal{G} . Denote by S the set of sources and sinks in $\mathcal{T}_{\mathcal{G}}$. Let h be a function that maps every vertex \mathbf{e} in $V - S$ to a new arrow $v_e \xrightarrow{e} v'_e$. Define the sets:

$$V' = \bigcup_{\mathbf{e} \in \overline{V} - S} \{v_e, v'_e\} \quad \text{and} \quad E' = \bigcup_{\mathbf{e} \in \overline{V} - S} \{h(\mathbf{e})\} = \bigcup_{\mathbf{e} \in \overline{V} - S} \{e\}.$$

Then, $\vec{\mathcal{G}} = (V, E)$ is such that $V = (\overline{V} - S) \cup V'$ and $E = \overline{E} \cup E'$. For every arrow $\alpha \in \overline{E}$ such that $s(\alpha) = \mathbf{e}$, the corresponding arrow $\alpha \in E$ satisfies $s(\alpha) = v_e$; otherwise, if $\alpha \in \overline{E}$ is such that $t(\alpha) = \mathbf{e}$, then $\alpha \in E$ satisfies $t(\alpha) = v'_e$. The underlying graph of $\vec{\mathcal{G}}$ (i.e., without considering the direction of the arrows) is the snake graph \mathcal{G} .

Theorem 3.21. Let \mathcal{G} be a snake graph. The set of perfect matchings $\text{Match}(\mathcal{G})$ of \mathcal{G} is in bijection with the set of k -routes from s to t in $\mathcal{T}_{\mathcal{G}}$.

Proof. According to Lemma 3.14, every perfect matching $P \in \text{Match}(\mathcal{G})$ gives rise to a k -route from s to t in $\mathcal{T}_{\mathcal{G}}$. It is sufficient to prove that for every k -route R , we can obtain a perfect matching P_R and that different k -routes give rise to different perfect matchings. We think of $\mathcal{T}_{\mathcal{G}}$ as the oriented contracted snake graph associated to \mathcal{G} and consider the decontraction process and the notation described in Remark 3.20. Consider a k -route R from s to t in $\mathcal{T}_{\mathcal{G}}$. We consider the following subsets of arrows and vertices in $\mathcal{T}_{\mathcal{G}}$:

- (1) Let $T \subseteq \overline{E}$ be the set of all arrows α in $\mathcal{T}_{\mathcal{G}}$ such that α belongs to a path p of R .
- (2) Let $U \subseteq \overline{V} - S$ be the set of all non-source or non-sink vertices \mathbf{e} in $\mathcal{T}_{\mathcal{G}}$ such that \mathbf{e} does not belong to a path of R .

We claim that the edges associated to T and U obtained after the decontraction process form a perfect matching P_R of \mathcal{G} . First, we will show that all vertices in \mathcal{G} belong to an edge of the decontraction process of $T \cup U$. This is evident because the vertices of $\mathcal{T}_{\mathcal{G}}$ are sources, sinks, or contractions of edges. In the first two cases, for every source s_i and sink t_i there exists a path in the k -route R starting at s_i and ending at t_i . Therefore, all sources and sinks belong to the edges obtained by the decontraction process of T . In the third case, every vertex \mathbf{e} obtained by contraction of an edge belongs to the edges obtained by the decontraction process of T , provided \mathbf{e} belongs to a path of R ; or \mathbf{e} belongs to the edges obtained by the decontraction process of U , in case \mathbf{e} does not belong to a path of R .

Now, we aim to show that for any two distinct edges e and e' in the decontraction process of $T \cup U$, e and e' do not share common vertices. For every path

$$p_i = s_i \xrightarrow{\alpha_1} \mathbf{e}_1 \xrightarrow{\alpha_2} \mathbf{e}_2 \xrightarrow{\alpha_3} \dots \xrightarrow{\alpha_{l-1}} \mathbf{e}_{l-1} \xrightarrow{\alpha_l} t_i$$

in R , we obtain the following edges when we apply the decontraction process.

$$s_i \xrightarrow{\alpha_1} v_{\mathbf{e}_1} \xrightarrow{e_1} v'_{\mathbf{e}_1} \xrightarrow{\alpha_2} v_{\mathbf{e}_2} \xrightarrow{e_2} v'_{\mathbf{e}_2} \xrightarrow{\alpha_3} \dots \xrightarrow{\alpha_{l-1}} v_{\mathbf{e}_{l-1}} \xrightarrow{e_{l-1}} v'_{\mathbf{e}_{l-1}} \xrightarrow{\alpha_l} t_i$$

A diagram showing a vertex v_e on the left and a vertex v'_e on the right. They are connected by a horizontal red line segment labeled e . From v_e , two black lines extend outwards to the left, one upwards and one downwards. From v'_e , two black lines extend outwards to the right, one upwards and one downwards.

Finally, let us consider two distinct k -routes, denoted as R and R' . We observe that their corresponding perfect matchings, namely P_R and $P_{R'}$, are distinct. This follows directly from the existence of an arrow α in a path of R that is absent in any path of R' . According to the definitions of P_R and $P_{R'}$, the edge corresponding to α is included in P_R but not in $P_{R'}$. Consequently, P_R and $P_{R'}$ differ. \square

Example 3.23. Consider the snake graph of Example 3.3. Its contracted snake graph is depicted as follows.

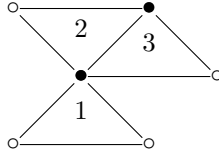
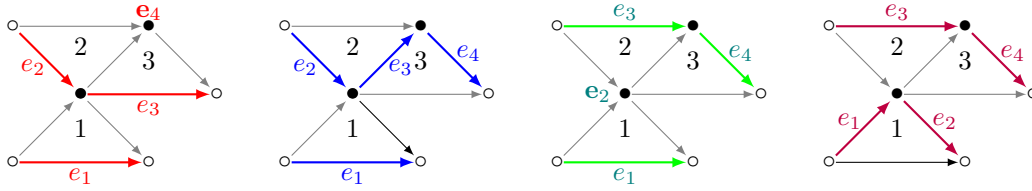


Diagram of a directed graph \mathcal{T}_G with nodes s_1, s_2, t_1, t_2 and two internal nodes. Edges are labeled 1, 2, 3.

$$M_{st} = \begin{pmatrix} 2 & 2 \\ 1 & 3 \end{pmatrix}.$$

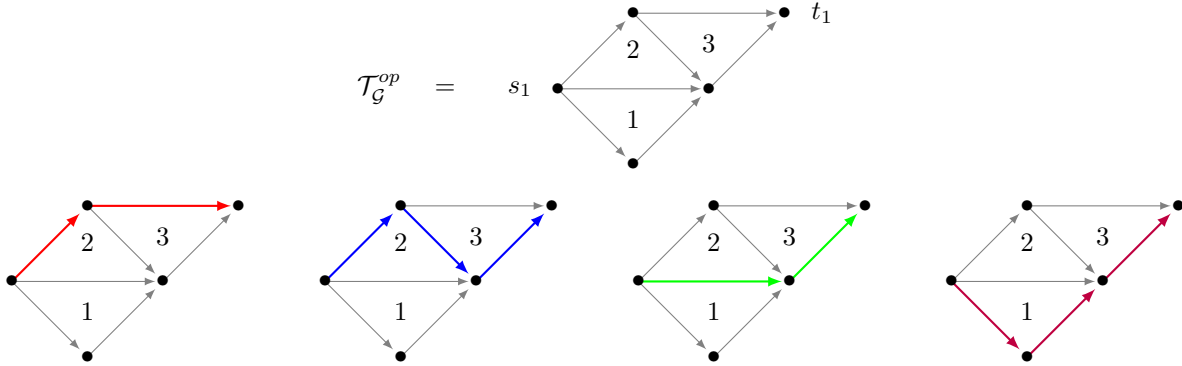
Figure 1 shows four diagrams of a 2x2 grid graph, each with a different edge coloring. The edges are labeled e_1, e_2, e_3, e_4 . In (a), the edges are colored red. In (b), the edges are colored blue. In (c), the edges are colored green. In (d), the edges are colored red.



We observe that when examining the contracted snake graph corresponding to a perfect matching, it aligns with the k -route immediately below it. Likewise, applying the decontraction process to a k -route yields the perfect matching that lies above it.

Remark 3.24. Note that in Definition 3.17, the assignment of northern and southern contractions to odd and even indices is arbitrary. One could equally well consider the opposite assignment, where northern contractions are associated with even indices and southern contractions with odd indices. Although the resulting contracted snake graphs are different with potentially varying numbers of sources and sinks, the number of routes remains invariant. Moreover, the bijection between the perfect matchings and the routes of the contracted snake graph obtained by this opposite assignment can still be established. Throughout this paper, we will consider both constructions, as the combinatorial properties of one may be more convenient than the other, depending on the desired formulas for counting paths or routes.

Example 3.25. Consider the snake graph of Example 3.3. Its contracted snake graph \mathcal{T}_G is depicted in Example 3.23. If we consider the opposite assignment, where northern contractions are associated with even indices and southern contractions with odd indices, we obtain the following triangular snake graph \mathcal{T}_G^{op} and corresponding routes



4. FIBONACCI IDENTITIES AND HANKEL MATRICES

4.1. Identities in straight snake graphs. In this section, our primary objective is to identify matrices exhibiting a certain form of "equivalence" to particular families of Hankel matrices based on lattice paths. This exploration intends to present instances where simpler acyclic graphs can be identified. These graphs provide a more straightforward approach for determining the entries of the path matrix and computing specific determinants. In particular, in this subsection we work with a special class of snake graphs known as ladder graphs before addressing the general case. We fix the following notation:

Definition 4.1. A ladder graph L_n is defined as a straight snake graph with n tiles.

Following the construction from the previous section, in the next proposition, we consider a directed acyclic graph that contains as a subgraph the triangular snake graph associated with a ladder graph. Later, we will see that this subgraph preserves the same number of paths as the graph considered in the proposition derived from Aztec diamonds.

Proposition 4.2. Let C be the sequence of Catalan numbers C_n and let F_n be the n -th Fibonacci number. Then the following relationship holds:

$$\det(H_k(C) + H'_k(C)) = F_{2k+1},$$

where $H_k(C)$ and $H'_k(C)$ are the Hankel matrices of the Catalan numbers.

Proof. The main idea of this proof is to identify a suitable graph that enables us to employ Lemma 2.1, thereby equating the requested determinant with the number of paths in the said graph. Notably, each component of the matrix counts the number of lattice paths in \mathbb{Z}^2 that start at $(0, 0)$ and end at $(2n, 0)$, and the number of lattice paths that start at $(0, 0)$ and end at $(2n + 2, 0)$. Observe that in the acyclic-directed graph in Figure 6, there are precisely $C_{i+j-2} + C_{i+j-1}$ paths from the vertex s_i to the vertex t_j .

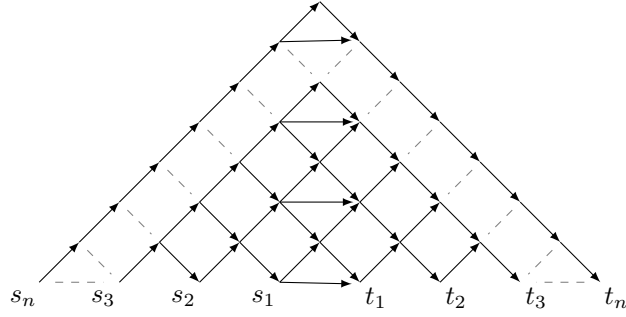
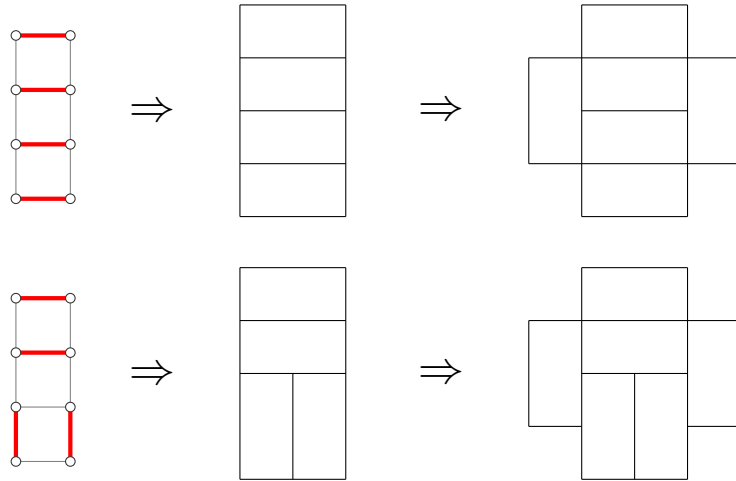
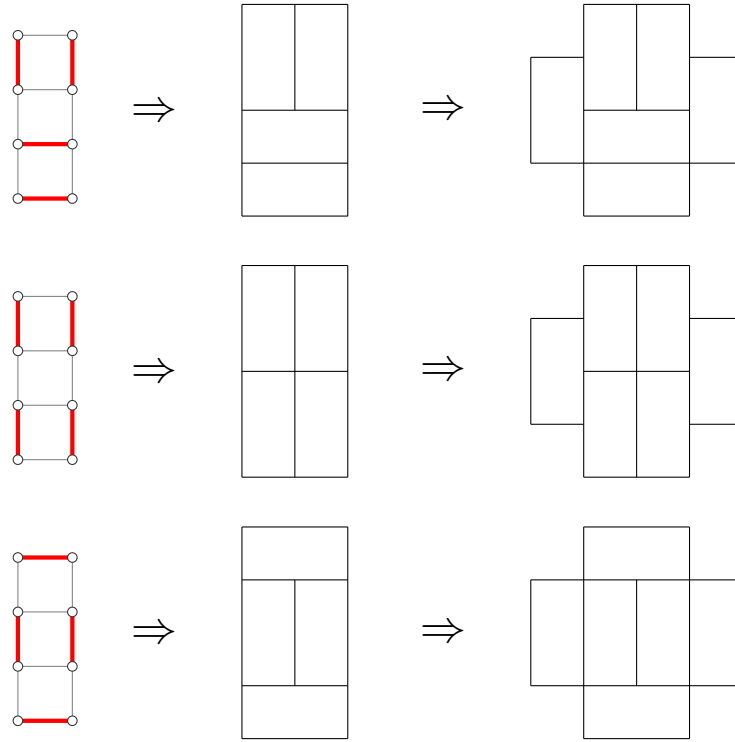


FIGURE 6. Catalan acyclic-directed graph associated to n -routes.

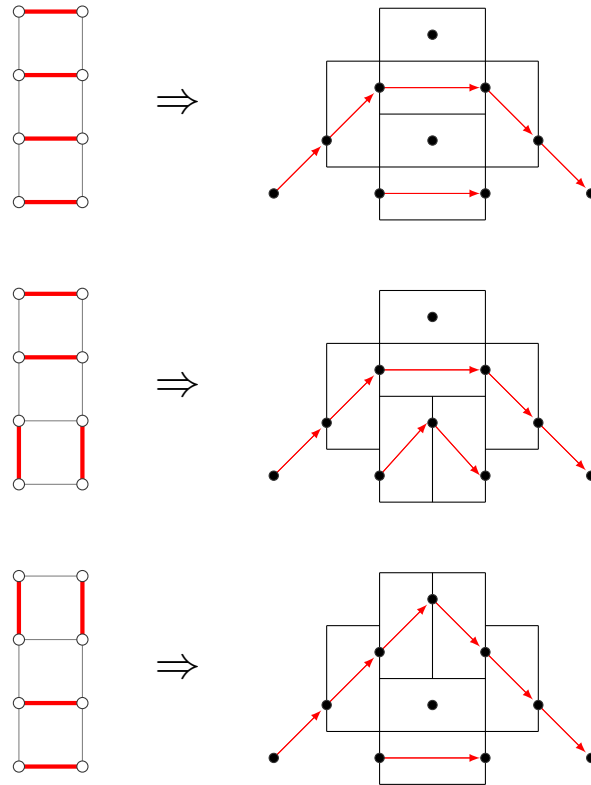
Therefore, the requested determinant counts the n -routes from s to t in the aforementioned graph. These paths correspond to the Aztec diamonds defined in 2.1, which, in turn, are linked to perfect matchings. Consequently, the result follows immediately. \square

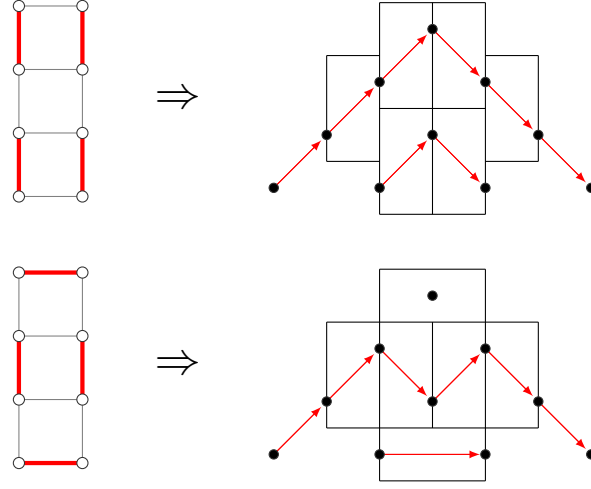
Example 4.3. For the five perfect matchings of L_3 we obtain the following domino tiling of $Az(2)$:





Therefore, we have the following routes for each perfect matching.





Therefore, the acyclic-directed graph in Figure 7 is constructed by superimposing every one of the previously obtained routes.

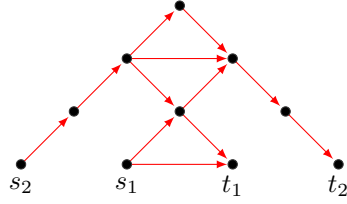


FIGURE 7. Acyclic-directed graph constructed by superimposing 2-routes.

The acyclic-directed graph in Figure 7 allows us to add arrows as long as they do not affect the number of 2-routes. For instance, we can add two arrows as shown in Figure 8 (one ending at vertex s_1 and another starting at vertex t_1). This is because 2-routes are a collection of two vertex-disjoint paths. Since the path from s_1 to t_1 shares vertices with the new arrows, the path from s_2 to t_2 cannot intersect it.

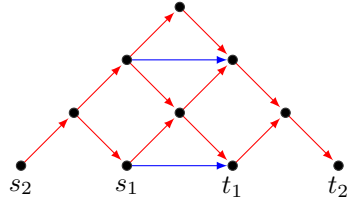


FIGURE 8. Catalan acyclic-directed graph associated to 2-routes.

To find the entries of the path matrix, the color of the horizontal arrows was changed to blue in Figure 8. If we want to see the paths from vertex s_i to vertex t_j , then we can see that the number of paths that use a blue edge is C_{i+j-2} , and the number of paths that do not use those blue edges is C_{i+j-1} . Therefore, the path matrix is

$$M_2 = \begin{pmatrix} C_0 + C_1 & C_1 + C_2 \\ C_1 + C_2 & C_2 + C_3 \end{pmatrix} = \begin{pmatrix} 2 & 3 \\ 3 & 7 \end{pmatrix}$$

where it can easily be verified that $\det(M_2) = 5$.

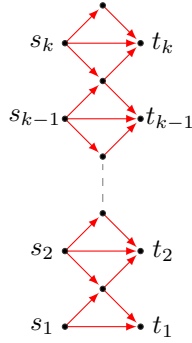
Proposition 4.4. Let $M_{st} = (m_{ij})_{1 \leq i, j \leq k}$ be the path matrix associated to the triangular snake graph of the vertical ladder graph L_{2k-1} , $k \geq 1$, and let F_n be the n -th Fibonacci number. Then the following relationship holds

$$\det M_{st} = F_{2k+1},$$

where

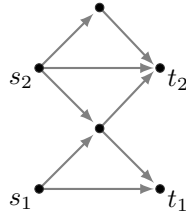
$$m_{ij} = \begin{cases} F_3 = 2 & \text{if } i = j = 1; \\ F_4 = 3 & \text{if } i = j \in \{2, \dots, k\}; \\ F_2 = 1 & \text{if } i = j + 1 \text{ or } i = j - 1; \\ F_0 = 0 & \text{otherwise.} \end{cases}$$

Proof. Consider the vertical ladder graph L_{2k-1} . We obtain the following triangular snake graph $\mathcal{T}_{L_{2k-1}}$

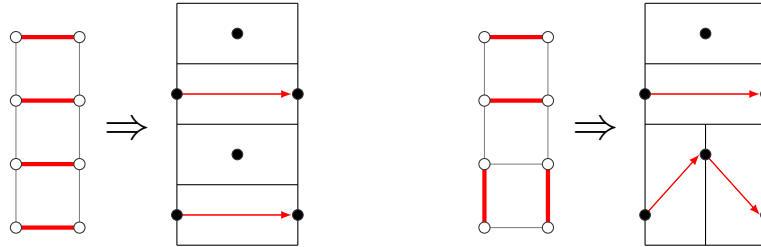


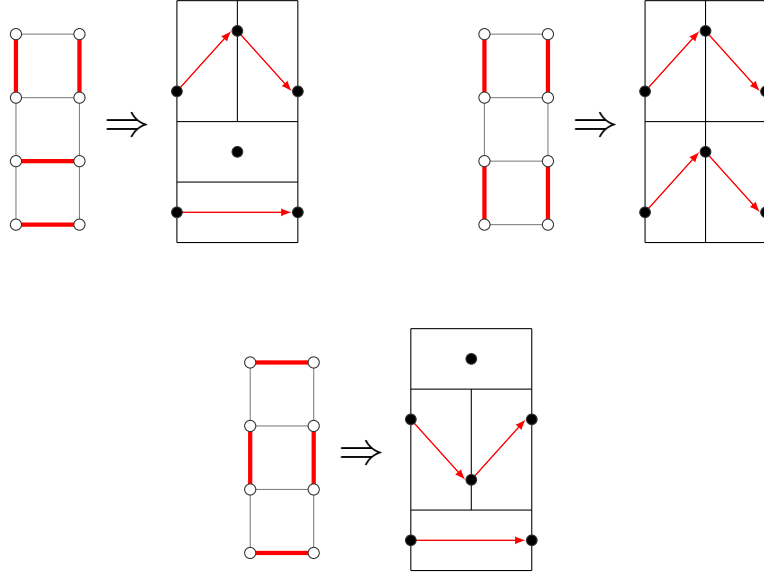
From a direct inspection we can see that the number m_{ii} of paths p_i from s_i to t_i is equal to 3 if $i \in \{2, 3, \dots, k\}$ and equal to 2 if $i = 1$. In addition, the number m_{ij} of paths from s_i to t_j is equal to 1 if $|i - j| = 1$ and equal to 0 if $|i - j| > 1$. Then, using Lemma 2.1 we conclude the proposition. \square

Example 4.5. Consider the ladder graph L_3 of the Example 4.3. The triangular snake graph can be represented as follows:



We obtain the following perfect matchings and their corresponding 2-routes





Then comparing Proposition 4.2 with Proposition 4.4 we obtain

$$\begin{vmatrix} C_0 + C_1 & C_1 + C_2 \\ C_1 + C_2 & C_2 + C_3 \end{vmatrix} = \begin{vmatrix} 2 & 3 \\ 3 & 7 \end{vmatrix} = F_5 = \begin{vmatrix} 2 & 1 \\ 1 & 3 \end{vmatrix} = \begin{vmatrix} F_3 & F_2 \\ F_2 & F_4 \end{vmatrix}.$$

Remark 4.6. Based on the earlier finding, we can discern that the Hankel matrix discussed in Proposition 4.2 shares an identical determinant with the matrix presented in Proposition 4.4. Although both matrices exhibit similarities in terms of determinants, it is noteworthy to highlight the contrast in their components. The former matrix encompasses a total of k^2 non-zero entries, while the latter matrix boasts a more compact structure with only $3k - 2$ non-zero entries.

This discrepancy in the number of non-zero entries underscores a notable difference in the structures of these matrices. Exploring such differences might provide valuable insights into the underlying structures and relationships in Hankel matrices and contribute to the broader understanding of their significance in mathematical theory and applications.

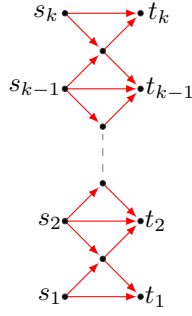
Proposition 4.7. Let $M_{st} = (m_{ij})_{1 \leq i, j \leq k}$ be the path matrix associated to the triangular snake graph of the vertical ladder graph L_{2k-2} , where $k \geq 1$. Let C be the sequence of Catalan numbers C_n and let F_n be the n -th Fibonacci number. Then the following relationship holds:

$$\det M_{st} = F_{2k} = \det (H_k(C) + H'_k(C) - E_{k,k}),$$

where $E_{i,j}$ is the matrix whose (i, j) -th entry is 1 and all other entries are zero, $H_k(C)$ and $H'_k(C)$ are the Hankel matrices of the Catalan numbers and

$$m_{ij} = \begin{cases} F_3 = 2 & \text{if } i = j = 1 \text{ or } i = j = k; \\ F_4 = 3 & \text{if } i = j \in \{2, \dots, k-1\}; \\ F_2 = 1 & \text{if } i = j + 1 \text{ or } i = j - 1; \\ F_0 = 0 & \text{otherwise.} \end{cases}$$

Proof. This follows by the same method as in the proofs of Propositions 4.2 and 4.4, considering the ladder graph L_{2k-2} . The following is the triangular snake graph associated to L_{2k-2} .



An easy computation shows that the path matrix of the previous triangular snake graph is the desired one. \square

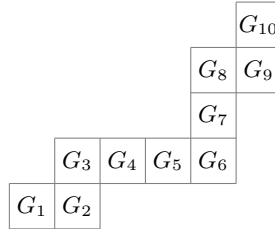
4.2. Some identities in not straight snake graphs. Building on our previous results regarding Fibonacci numbers and ladder graphs, this chapter extends our analysis to more general snake graphs. We introduce a new notation to define a snake graph in terms of the length of each maximal straight subgraph within this graph, allowing us to study their properties and relationships with Fibonacci numbers.

Definition 4.8. Given a snake graph \mathcal{G} , a *chain* \mathcal{G}_{ij} is a subgraph of \mathcal{G} that forms a maximal ladder graph. That is, there are no other ladder graphs within \mathcal{G} that contain \mathcal{G}_{ij} , and \mathcal{G}_{ij} consists of the tiles G_k , where $i \leq k \leq j$. The *length* $l(\mathcal{G}_{ij})$ of a chain \mathcal{G}_{ij} is defined as the number of tiles it contains, *i.e.*, $l(\mathcal{G}_{ij}) = j - i + 1$.

Based on Definition 4.8, we can describe a snake graph using its horizontal and vertical chains. We denote by $\mathcal{G}_h(l_1, l_2, \dots, l_k)$ the snake graph in which l_i represents the length of the horizontal chains when i is odd, and the length of the vertical chains when i is even. Conversely, $\mathcal{G}_v(l_1, l_2, \dots, l_k)$ denotes the snake graph where l_i represents the length of the vertical chains if i is odd, and the length of the horizontal chains if i is even. The concept of a chain can be analogously defined for triangular snake graphs.

Remark 4.9. The only snake graph that contains a chain of length 1 is the one formed by a single tile, denoted as $\mathcal{G} = G_1 = \mathcal{G}_h(1) = \mathcal{G}_v(1)$. In all other cases, the chains have a length of at least 2. However, in some computations (see Lemma 4.11), initial chains of length 0 or 1 may appear. By convention, we define $\mathcal{G}_h(0, l_2, \dots, l_k) = \mathcal{G}_v(l_2 - 1, l_3, \dots, l_k)$ and $\mathcal{G}_h(1, l_2, \dots, l_k) = \mathcal{G}_v(l_2, l_3, \dots, l_k)$. Similarly, we set $\mathcal{G}_v(0, l_2, \dots, l_k) = \mathcal{G}_h(l_2 - 1, l_3, \dots, l_k)$ and $\mathcal{G}_v(1, l_2, \dots, l_k) = \mathcal{G}_h(l_2, l_3, \dots, l_k)$.

Example 4.10. The snake graph $\mathcal{G}_h(2, 2, 4, 3, 2, 2)$ is illustrated below:



This snake graph consists of 3 horizontal chains:

$$\begin{aligned}\mathcal{G}_{1,2} &= \{G_1, G_2\}, \\ \mathcal{G}_{3,6} &= \{G_3, G_4, G_5, G_6\}, \\ \mathcal{G}_{8,9} &= \{G_8, G_9\},\end{aligned}$$

and 3 vertical chains:

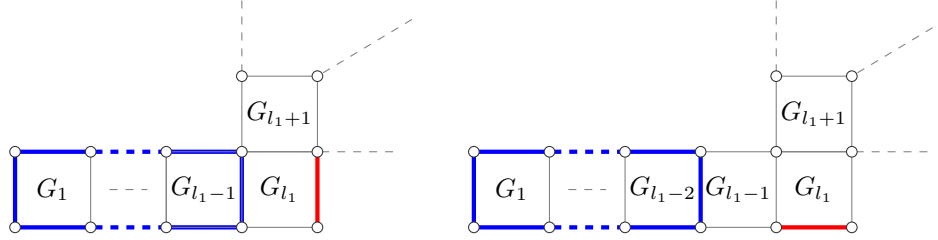
$$\begin{aligned}\mathcal{G}_{2,3} &= \{G_2, G_3\}, \\ \mathcal{G}_{6,8} &= \{G_6, G_7, G_8\}, \\ \mathcal{G}_{9,10} &= \{G_9, G_{10}\}.\end{aligned}$$

This chain description allows for recursive combinatorial counting using Fibonacci numbers, as illustrated in the following lemma.

Lemma 4.11. Let \mathcal{G} be a snake graph represented by $\mathcal{G}_h(l_1, l_2, \dots, l_k)$, where $l_i \geq 2$ for all $i \in \{1, \dots, k\}$. The number of perfect matchings $m(\mathcal{G})$ of \mathcal{G} is given by the recurrence relation:

$$m(\mathcal{G}) = F_{l_1} m(\mathcal{G}_v(l_2 - 1, l_3, \dots, l_k)) + F_{l_1+1} m(\mathcal{G}_v(l_2 - 2, l_3, \dots, l_k)).$$

Proof. We classify all perfect matchings of the snake graph $\mathcal{G} = \mathcal{G}_h(l_1, l_2, \dots, l_k)$ by considering the edge incident to the lower right vertex of the tile G_{l_1} . This edge can either be a vertical or a horizontal edge, as illustrated in the following figure:



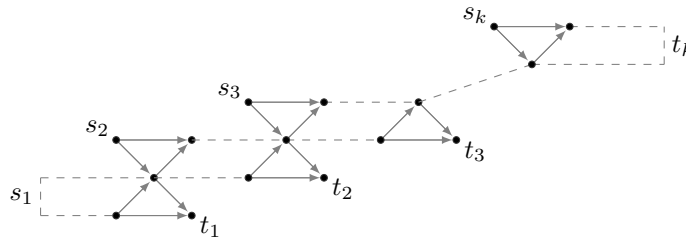
If a perfect matching contains the vertical edge, then the edges on the left part of the snake graph are chosen in $m(L_{l_1-1}) = F_{l_1+1}$ ways, and the edges of the remaining part of the snake graph are chosen in $m(\mathcal{G}_v(l_2 - 2, l_3, \dots, l_k))$ ways. Analogously, for a perfect matching that contains the horizontal edge, the edges on the left part of the snake graph are chosen in $m(L_{l_1-2}) = F_{l_1}$ ways, and the edges of the remaining part of the snake graph are chosen in $m(\mathcal{G}_v(l_2 - 1, l_3, \dots, l_k))$ ways. Therefore, the total number of perfect matchings $m(\mathcal{G})$ is given by the recurrence:

$$m(\mathcal{G}) = F_{l_1} m(\mathcal{G}_v(l_2 - 1, l_3, \dots, l_k)) + F_{l_1+1} m(\mathcal{G}_v(l_2 - 2, l_3, \dots, l_k)),$$

as desired. \square

Remark 4.12. As a preliminary observation, we note that a recurrence for $m(\mathcal{G}_v(l_1, l_2, \dots, l_k))$ can be derived in a manner analogous to the one presented in Lemma 4.11. This is because $\mathcal{G}_v(l_1, l_2, \dots, l_k)$ is a reflection of $\mathcal{G}_h(l_1, l_2, \dots, l_k)$, implying that both graphs are structurally identical, just mirrored. Consequently, we have $m(\mathcal{G}_v(l_1, l_2, \dots, l_k)) = m(\mathcal{G}_h(l_1, l_2, \dots, l_k))$. Additionally, for any snake graph, the number of perfect matchings can be expressed as a sum of products of Fibonacci numbers. In § 4.1, we observed that the entries of the path matrix for the triangular snake graph associated with a ladder graph are Fibonacci numbers. This leads us to inquire whether it is possible to express the entries of the path matrices for general snake graphs in terms of Fibonacci-like expressions.

Proposition 4.13. Let $M_{st} = (m_{ij})_{1 \leq i, j \leq k}$ be the path matrix associated to the following triangular snake graph:



derived from the snake graph $\mathcal{G}_h(l_1, 2, l_2, 2, \dots, 2, l_k)$ such that edge contraction of the $k-1$ vertical chains results in the hourglass graphs \mathbb{X}_i , $i \in \{1, \dots, k-1\}$. Then, the elements of M_{st} are given by:

$$m_{ij} = \begin{cases} F_{l_{i+1}} F_{l_{j+1}} \prod_{r=i+1}^{j-1} F_{l_r} & \text{if } i < j; \\ F_{l_i+2} & \text{if } i = j; \\ F_2 & \text{if } i = j+1; \\ F_0 & \text{otherwise.} \end{cases}$$

Proof. Since the vertical chains of the snake graph $\mathcal{G}_h(l_1, 2, l_2, 2, \dots, 2, l_k)$ are all of length two, and their edge contraction results in an hourglass graph, the number of paths from vertex s_i to vertex t_i , for $i \in \{1, \dots, k\}$, is equal to the Fibonacci number F_{l_i+2} , as the graph corresponds to a triangular snake graph associated to a ladder graph L_{l_i} . On the other hand, there is only $F_2 = 1$ path from vertex s_i to vertex t_j if $i - j = 1$, and $F_0 = 0$ if $i - j > 1$.

Finally, to address the remaining case, we note that a path from s_i to s_j for $i < j$ must pass through the necks of the intermediate hourglass graphs $\mathbb{X}_i, \dots, \mathbb{X}_{j-1}$, so does not pass through the arrows incident to the source or sink vertices of these graphs. Specifically, there are F_{l_i+1} paths from s_i to the neck n_i of \mathbb{X}_i , F_{l_j+1} paths from n_{j-1} to t_j , and F_{l_r} paths from n_{r-1} to n_r for each $r \in \{i+1, \dots, j-1\}$. Therefore,

the total number of paths is $m_{ij} = F_{l_i+1} F_{l_j+1} \prod_{r=i+1}^{j-1} F_{l_r}$, as desired. \square

Remark 4.14. In Proposition 4.13, the associated triangular snake graph can be obtained by applying either the contraction defined in Definition 3.17 or the opposite contraction considered in Remark 3.24. For general snake graphs where not all edge contractions of vertical chains result in hourglass graphs, it is still possible to express path matrices in terms of Fibonacci numbers. However, these cases involve applying both the original and opposite contractions simultaneously. Consequently, some entries in the path matrices may be determinants of smaller path matrices, which themselves can be described using Fibonacci numbers.

In § 4.1, we examined path matrices whose entries were expressed in terms of Fibonacci or Catalan numbers, with determinants also yielding Fibonacci numbers. We now explore an example where the determinant corresponds to a different well-known numerical sequence.

Proposition 4.15. Let P_n be the n -th Pell number defined recursively by $P_n = 2P_{n-1} + P_{n-2}$ for $P_0 = 0$, $P_1 = 1$ and $n \geq 2$. Let $M_k = (m_{ij})$ and $M'_k = (m'_{ij})$ be the $k \times k$ matrices defined as follows:

$$m_{ij} = \begin{cases} F_5 & \text{if } i = j = 1; \\ F_5 + F_3 & \text{if } i = j \in \{2, \dots, k\}; \\ F_4 F_3 & \text{if } i = 1 \text{ and } j > 1; \\ (F_4 + F_2) F_3 & \text{if } i \neq 1 \text{ and } i < j; \\ F_2 & \text{if } i = j + 1; \\ F_0 & \text{otherwise.} \end{cases}$$

and

$$m'_{ij} = \begin{cases} F_5 & \text{if } i = j = 1; \\ F_5 + F_3 & \text{if } i = j \in \{2, \dots, k-1\}; \\ F_4 F_3 & \text{if } i = 1 \text{ and } 1 < j < k; \\ (F_4 + F_2) F_3 & \text{if } i \neq 1, j \neq k \text{ and } i < j; \\ F_4 + F_2 & \text{if } 1 < i < k \text{ and } j = k; \\ F_4 & \text{if } i \in \{1, k\} \text{ and } j = k; \\ F_2 & \text{if } i = j + 1; \\ F_0 & \text{otherwise.} \end{cases}$$

Then,

$$\det M_k = P_{2k+1} \quad \text{and} \quad \det M'_k = P_{2k}.$$

Proof. Consider the snake graph \mathcal{G} associated to the continued fraction $[2, 2, \dots, 2, 2]$. This snake graph consists of $2k - 1$ chains, each of length 3; that is, $\mathcal{G} = \mathcal{G}_h(\underbrace{3, 3, \dots, 3, 3}_{(2k-1)\text{-times}})$. From a direct inspection of Figure 9, we can observe that the matrix M_k corresponds to the path matrix associated to the triangular snake graph $\mathcal{T}_{\mathcal{G}}$.

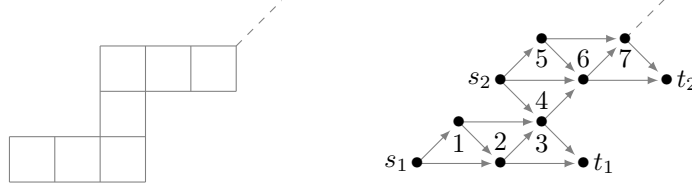
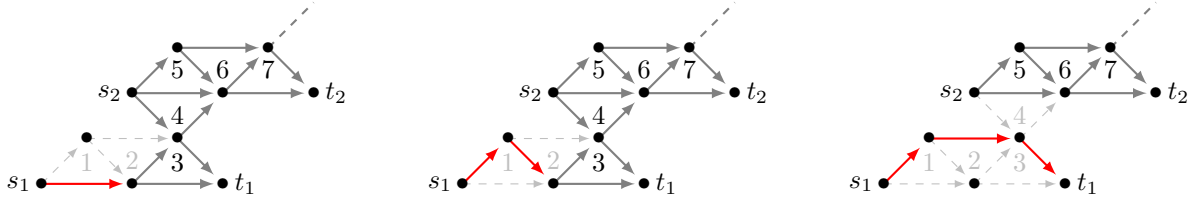


FIGURE 9. Pell Snake graph and its corresponding triangular snake graph.

Furthermore, by directly examining the routes in $\mathcal{T}_{\mathcal{G}}$, we observe that the paths from s_1 to t_1 fall into one of the following three cases:



The first two cases (from left to right) correspond to the number of routes in the triangular snake graph associated to $\mathcal{G}_v(\underbrace{3, 3, \dots, 3, 3}_{(2k-2)\text{-times}})$, while the remaining case corresponds to the number of routes in the triangular snake graph associated to $\mathcal{G}_h(\underbrace{3, 3, \dots, 3, 3}_{(2k-3)\text{-times}})$. Therefore, the number of routes in $\mathcal{T}_{\mathcal{G}}$ (or perfect

matchings in \mathcal{G}) satisfies the same recurrence relation as the Pell numbers. Similarly, if we consider the continued fraction $[2, 2, \dots, 2, 2]$, the associated path matrix is M'_k , whose determinant corresponds to the previously mentioned Pell number. Thus, the desired result is proved. \square

Example 4.16. Consider the snake graphs \mathcal{G}' and \mathcal{G} associated to the continued fractions $[2, 2, 2, 2, 2]$ and $[2, 2, 2, 2, 2, 2]$, respectively. The number of perfect matchings of \mathcal{G}' and \mathcal{G} are given by

$$m(\mathcal{G}') = \det M'_3 = \begin{vmatrix} F_5 & F_4 F_3 & F_4 \\ F_2 & F_5 + F_3 & F_4 + F_2 \\ F_0 & F_2 & F_4 \end{vmatrix} = P_6 = 70,$$

and

$$m(\mathcal{G}) = \det M_3 = \begin{vmatrix} F_5 & F_4 F_3 & F_4 F_3 \\ F_2 & F_5 + F_3 & (F_4 + F_2) F_3 \\ F_0 & F_2 & F_5 + F_3 \end{vmatrix} = P_7 = 169.$$

5. FUTURE WORK

This work has showed that, for all snake graphs, the number of perfect matchings can be expressed as a sum of products of Fibonacci numbers. Additionally, we have explored how certain well-known sequences, such as the Fibonacci and Pell sequences, can be characterized through determinants of matrices with Fibonacci number entries. A natural question arises: can other sequences be described similarly? For

instance, the Fibonacci and Pell numbers are particular cases within the broader Markov sequence. It would be interesting to study whether there are families of matrices that can effectively describe this sequence in an analogous manner.

Furthermore, previous works such as [23] and [24] established a relationship between the continued fraction associated with a snake graph, the number of perfect matchings, and the framework of cluster algebras. Specifically, if \mathcal{G} is the snake graph of a cluster variable within a cluster algebra arising from a surface, then each cluster variable \mathbf{x} is represented by a formula involving the perfect matchings of \mathcal{G} . Through the bijections introduced in this paper, we can reinterpret these expressions as products of arrow labels within paths of the k -route associated with a perfect matching, combined with labels of contraction edge vertices that are not part of any path in the route. This suggests a potential avenue for further exploration, where such combinatorial interpretations may offer new insights into the algebraic structures underlying cluster variables and related sequences.

6. ACKNOWLEDGMENTS

I would like to express my sincere gratitude to Alfredo Nájera Chávez for his invaluable comments, suggestions, and corrections on earlier drafts of this work. Additionally, I thank Timothy Magee for his insightful observations, particularly regarding the use of Hankel notation in Proposition 4.2. Their contributions have significantly improved the quality of this paper.

REFERENCES

- [1] F. Ardila, *Algebraic and Geometric Methods in Enumerative Combinatorics*. Boca Raton, CRC Press: Handbook of enumerative combinatorics, 09 2015.
- [2] F. Ardila and R. Stanley, “Tilings*,” *The Mathematical Intelligencer*, vol. 32, pp. 32–43, 08 2010. [Online]. Available: <https://doi.org/10.1007/s00283-010-9160-9>
- [3] A. Benjamin, N. Cameron, and J. Quinn, “Fibonacci determinants - a combinatorial approach,” *The Fibonacci Quarterly*, vol. 45, 12 2005.
- [4] L. M. Bregman, “Some properties of nonnegative matrices and their permanents,” *Soviet Math. Dokl.*, vol. 211, pp. 27–30, 06 1973.
- [5] S. Butler, J. Ekstrand, and S. Osborne, *Counting Tilings by Taking Walks in a Graph*. Springer International Publishing, 2020, pp. 153–176. [Online]. Available: https://doi.org/10.1007/978-3-030-37853-0_5
- [6] M. Ciucu, “Perfect matchings of cellular graphs,” *J. Algebraic Combinatorics*, vol. 5, p. 87–103, 04 1996.
- [7] N. Elkies, G. Kuperberg, M. Larsen, and J. Propp, “Alternating sign matrices and domino tilings,” *Journal of Algebraic Combinatorics*, vol. 1, pp. 111–132, 09 1992.
- [8] S.-P. Eu and T.-S. Fu, “A simple proof of the aztec diamond theorem,” *Electronic Journal of Combinatorics*, vol. 12, p. 8 pp., 01 2005.
- [9] M. Fisher and H. Temperley, “Dimer problem in statistical mechanics – an exact result,” *Philosophical Magazine*, vol. 68, p. 1061–1063, 6 1961.
- [10] N. Garnier and O. Ramaré, “Fibonacci numbers and trigonometric identities,” *Fibonacci Quart.*, pp. 1–7, 02 2008.
- [11] I. Gessel and X. Viennot, “Determinants, paths, and plane partitions,” *Preprint*, 1989.
- [12] P. W. Kasteleyn, “The statistics of dimers on a lattice i. the number of dimer arrangements on a quadratic lattice,” *Physica*, vol. 27, p. 1209–1225, 12 1961.
- [13] M. Katz and C. Stenson, “Tiling a $(2 \times n)$ -board with squares and dominoes,” *Journal of Integer Sequences*, vol. 12, 01 2009.
- [14] T. Koshy, *Fibonacci and Lucas Numbers with Applications*. New York: Pure and applied mathematics: a Wiley-Interscience series of texts, monographs, and tract, 2001.
- [15] J. Layman, “The hankel transform and some of its properties,” *Journal of Integer Sequences*, vol. 4, p. 11, 2001.
- [16] B. Lindström, “On the vector representations of induced matroids,” *Bulletin of the London Mathematical Society*, vol. 5, p. 85–90, 03 1973.
- [17] C. Melo, *Emparejamientos perfectos, álgebras de conglomerado y algunas de sus aplicaciones (Master’s thesis)*. Universidad Nacional de Colombia, Bogotá, Colombia, 2019.
- [18] G. Musiker, R. Schiffler, and L. Williams, “Positivity for cluster algebras from surfaces,” *Advances in Mathematics*, vol. 227, no. 6, pp. 2241–2308, 2011. [Online]. Available: <https://www.sciencedirect.com/science/article/pii/S0001870811001423>
- [19] —, “Bases for cluster algebras from surfaces,” *Compos. Math.*, vol. 149, no. 2, pp. 217–263, 2013.
- [20] N. Sloane, “The on-line encyclopedia of integer sequences,” *published electronically*, 1964. [Online]. Available: <https://oeis.org/>

- [21] R. Stanley, *Enumerative Combinatorics, Volume 2*. Cambridge Studies in Advanced Mathematics, vol. 62, Cambridge University Press: Cambridge, 1999.
- [22] —, *Catalan Numbers*. Cambridge University Press, 2015.
- [23] I. Çanakçı and R. Schiffler, “Snake graph calculus and cluster algebras from surfaces,” *Journal of Algebra*, vol. 382, pp. 240–281, 09 2013.
- [24] —, “Cluster algebras and continued fractions,” *Compositio Mathematica*, vol. 154, no. 3, p. 565–593, 08 2018.

CAROLINA MELO

DEPARTAMENTO DE MATEMÁTICAS, UNIVERSIDAD NACIONAL DE COLOMBIA - SEDE BOGOTÁ, AVE
CRA 30 #45-3, BOGOTÁ, COLOMBIA

e-mail: amelol@unal.edu.co